AD 295 723

Report No. 7

Seventh Quarterly Progress Report | *Covering the Period 1 July to 30 September 1962*

MICROWAVE FILTERS AND COUPLING STRUCTURES

Prepared for:

U.S. ARMY ELECTRONICS RESEARCH AND DEVELOPMENT LABORATORY
FORT MONMOUTH, NEW JERSEY

CONTRACT DA 36-039 SC 87398
FILE NO. 40553-PM-61-93-93
DA PROJECT 3A99-15-002-02-06
SCL-2101N (14 JULY 1961)

By: *B. M. Schiffman* *P. S. Carter, Jr.* *G. L. Matthaei*

STANFORD RESEARCH INSTITUTE

MENLO PARK, CALIFORNIA

October 1962

Report No. 7

Seventh Quarterly Progress Report | *Covering the Period 1 July to 30 September 1962*

MICROWAVE FILTERS AND COUPLING STRUCTURES

Prepared for:

U.S. ARMY ELECTRONICS RESEARCH AND DEVELOPMENT LABORATORY
FORT MONMOUTH, NEW JERSEY

CONTRACT DA 36-039 SC 87398
FILE NO. 40553-PM-61-93-93
DA PROJECT 3A99-15-002-02-06
SCL-2101N (14 JULY 1961)

By: *B. M. Schiffman* *P. S. Carter, Jr.* *G. L. Matthaei*

SRI Project No. 3527

Objective: To advance the state of the art in the field of microwave filters and coupling structures through applied research and development.

Approved:

G. L. Matthaei

G. L. MATTHAEI, MANAGER ELECTROMAGNETIC TECHNIQUES LABORATORY

D. R. Scheuch

D. R. SCHEUCH, DIRECTOR ELECTRONICS AND RADIO SCIENCES DIVISION

Copy No. 24

ABSTRACT

An exact method is presented for the design of band-stop filters consisting of stubs and quarter-wavelength connecting lines. Using this method a low-pass prototype circuit is chosen, and the transmission-line band-stop filter derived from the prototype will have a response that is an exact mapping of the prototype response. In theory the stop band can have any width, but if the stop band is very narrow the stub impedances become unreasonable. In such cases it is found to be desirable to replace the stubs by capacitively or inductively coupled resonators of reasonable impedance. This introduces an approximation but gives very good results. The design of filters having three-quarter-wavelength spacings between resonators is also discussed. This latter case is of interest for the design of waveguide band-stop filters where it has been found to be desirable to separate the resonators by three quarter-wavelengths in order to avoid interactions between the fringing fields at the coupling irises.

A review of the procedure employed in the establishment of the parameters and dimensions of magnetically tunable filters is given. Charts and graphs are presented which enable a designer to arrive at the dimensions of the circuit elements, including the ferrimagnetic resonators, in order to give a specified band-pass frequency response. Circuit structures are presented which appear or which have proved to be very promising for practical applications. Two typical examples are given of the design of two-resonator band-pass filters, one of which employs a waveguide and the other a strip-transmission-line coupling circuit. Finally, the performances of two side-wall-coupled strip-transmission-line filters, one containing two resonators and the other three, are discussed. The results are compared with a previous version of the two-resonator side-wall-coupled filter and with a previously developed overlapping line version.

CONTENTS

CONTENTS

ILLUSTRATIONS

ILLUSTRATIONS

TABLES

PURPOSE OF THE CONTRACT

This contract continues the work of Contracts DA 36-039 SC-64625, DA 36-039 SC-63232, and DA 36-039 SC-74862 to develop new design techniques for waveguide, strip-line, and coaxial-line microwave components, and to prepare a handbook on techniques for microwave filter design.

CONFERENCES AND TECHINICAL PAPERS

Conferences

On September 17 and 18, 1962 Mr. W. P. Dattilo of USAERDL visited Stanford Research Institute and discussed the course of this research with Dr. G. L. Matthaei, Dr. P. S. Carter, Jr., Mr. B. M. Schiffman and Dr. E. G. Cristal.

Technical Papers

Leo Young, "Prediction of Absorption Loss in Multilayer Interference Filters," *Jour. of the Optical Society of America*, vol. 52, pp. 753-761 (July 1962).

I INTRODUCTION

In Quarterly Progress Report 3 on this contract, an approximate method for the design of band-stop microwave filters was presented. This method was applicable to the design of either strip-line or waveguide band-stop filters having narrow stop bands (say, with stop bands of 10 percent bandwidth or less). In this report another design approach is developed which is exact, and which is applicable to the design of band-stop filters with either wide or narrow stop bands. However, in the case of narrow stop bands the stub impedances become impractical and it becomes necessary to use reactively coupled stubs (which introduce an approximation). However, even with this approximation, the accuracy is better than that obtained with the previous approximate procedure.

Another problem being studied on this project is means for designing electronically tunable microwave filters. In the past a study was made of the feasibility of using variable-capacitance diodes as voltage-controlled capacitors in filter circuits. In principle one can use capacitors to obtain voltage-tunable filters, but our studies showed that presently available capacitors have too low a Q to be of much use for voltage-tunable microwave filters, although they should be useful at lower frequencies. Other methods for electronic tuning which are being investigated are magnetically tunable filters using garnet resonators, and electronically tunable up-converters.

Work is continuing on the use of ferrimagnetic resonance in yttrium-iron-garnet resonators which provide means for designing filters that can be tuned by varying a dc-biasing magnetic field. This approach appears to hold considerable promise for electronic tuning applications at frequencies around 2 Gc or above. Using gallium-substituted yttrium-iron-garnet resonators which have a relatively low saturation magnetization, practical operation to frequencies around 1 Gc may be possible. Section III of this report covers our latest results on magnetically tunable filters.

II AN EXACT METHOD FOR SYNTHESIS OF MICROWAVE BAND-STOP FILTERS

A. GENERAL

Various techniques for the exact synthesis of microwave filters have existed for some time.[1,2,3,4,5*] In many cases these procedures have involved the synthesis of special transfer functions and then the determining of the filter elements from the transfer function. Although these procedures are mathematically very elegant, they have found little actual application in microwave engineering of the very tedious nature of the design process. However, one procedure, described by Ozaki and Ishii,[4] utilizes Kuroda's transformation[4] applied in a simple way to lumped-element, low-pass filters in order to design a certain type of transmission-line filter (which happens to be useful as a practical band-stop filter). In this case the use of a low-pass prototype along with Kuroda's transformation makes it possible to avoid most of the complexity inherent in many of the exact procedures.

Though the procedure of Ozaki and Ishii mentioned above[4] was described in mathematical form quite some time ago, no investigation of its practical nature appears to have been made. In this study the practical usefulness of this procedure as applied to band-stop filter design has been verified. In addition, tables of design equations have been prepared to make the results as easy as possible to use. With the aid of these tables a designer can obtain the filter designs he requires with a minimum of computational effort, and without having to go into the theory of how the equations were derived. However, the theory is discussed in Part F of this section.

In Part B of this section, there is presented a table of transmission-line filter formulas for filters with from one to five stubs, which are well-suited to band-stop filter design. The formulas have been derived by means of these new techniques. Each filter consists either of a tandem array of quarter-wavelength-long open-circuited transmission line

---

* References are listed at the end of the section.

shunt stubs (referred to stop-band center frequency ω_0) connected by quarter-wavelength-long transmission lines, or its dual in which open-circuited shunt stubs are replaced by short-circuited series stubs. The shunt stub arrangement is suitable for both balanced and unbalanced transmission-line filters operating in the TEM mode while the series stub arrangement is preferred for waveguide filters.

The characteristic impedance of each transmission-line section of the filter can be obtained by direct substitution of the element values of a low-pass ladder prototype filter into the formulas. The resulting band-stop filter response will have the same properties as that of the prototype (*i.e.*, Tchebyscheff ripples, etc.). An example of a three-resonator filter design is worked out and theoretical and measured results are given.

The method outlined, while theoretically exact, is on occasion limited by practical considerations; one in particular is the difficulty of constructing very-high- or very-low-impedance transmission lines such as would be required for very narrow stop bands. One must also contend with severe junction effects in very-low-impedance shunt-connected TEM lines and very-high-impedance series-connected waveguides. Still further, dissipation loss in very-high-impedance TEM lines could cause the stop-band response to deteriorate. A supplemental approximate technique that permits the use of moderate rather than very-high- or very-low-impedance stub lines with band-stop filters with narrow stop bands is described and illustrated in Part C of this section. In this case, the filter response necessarily departs somewhat from that predicted by the exact theory; however, the accuracy is markedly higher than that obtainable by the approximate theory for narrow-stop-band filter design discussed in Quarterly Progress Report 3 (see Ref. 10). However, the previously discussed design method has an advantage in that it does not require any steps in the main transmission line, while the method of this section does. The introduction of steps will mean additional manufacturing procedures, but in many cases the additional cost would be small.

There is no theoretical limitation on the number of $\lambda_0/4$ sections that can be used to separate each stub (or resonator) from its immediate neighbors, and in the case of waveguide filters it has been found to be desirable to separate the resonator irises by $3\lambda_0/4$ in order to avoid

undesirable interaction effects because of the fringing fields in the vicinity of the resonator irises. In Part D, design equations are given for filters having $3\lambda_0/4$ spacings between resonators, for the cases of two and three resonators.

The stop-band attenuation of low-pass filters can usually be improved by adding an inductor in series with one of the shunt capacitors, thus moving a pole of attenuation from infinite frequency to some finite frequency. For the special case of one pole at a finite frequency, the exact synthesis method of this section can be applied. Design formulas for this case are given in Part E.

In Part F the derivation of the formulas is fully described. The designer can thereby extend the table of formulas to greater values of n, which is the number of reactive elements in the prototype filter, and also derive formulas for transmission-line filters having connecting lines any desired odd number of quarter wavelengths long.

B. DESIGN FORMULAS AND THEIR USE

The relationship of the low-pass prototype response to that of the transmission line filter is illustrated in Fig. II B-1 and Fig. II B-2. One notes that the transmission-line filter response has, in addition to a low pass band, an infinite number of higher pass bands, each centered on an even multiple of the design frequency ω_0.

Table II B-1 relates specific frequencies of the lumped-element low-pass prototype filter in the ω'-plane to corresponding frequencies of the transmission-line filter in the ω-plane. The mapping function which maps the ω-plane into the ω'-plane is also given in this table. Two of the three critical frequencies of the low-pass prototype $\omega' = 0$ and $\omega' = \infty$ are fixed and the third ω_1' is determined by the low-pass prototype filter.

The formulas for transforming the prototype networks of Fig. II B-1 to the transmission line network of Fig. II B-2 (or to the dual of that network) are given in Table II B-2.

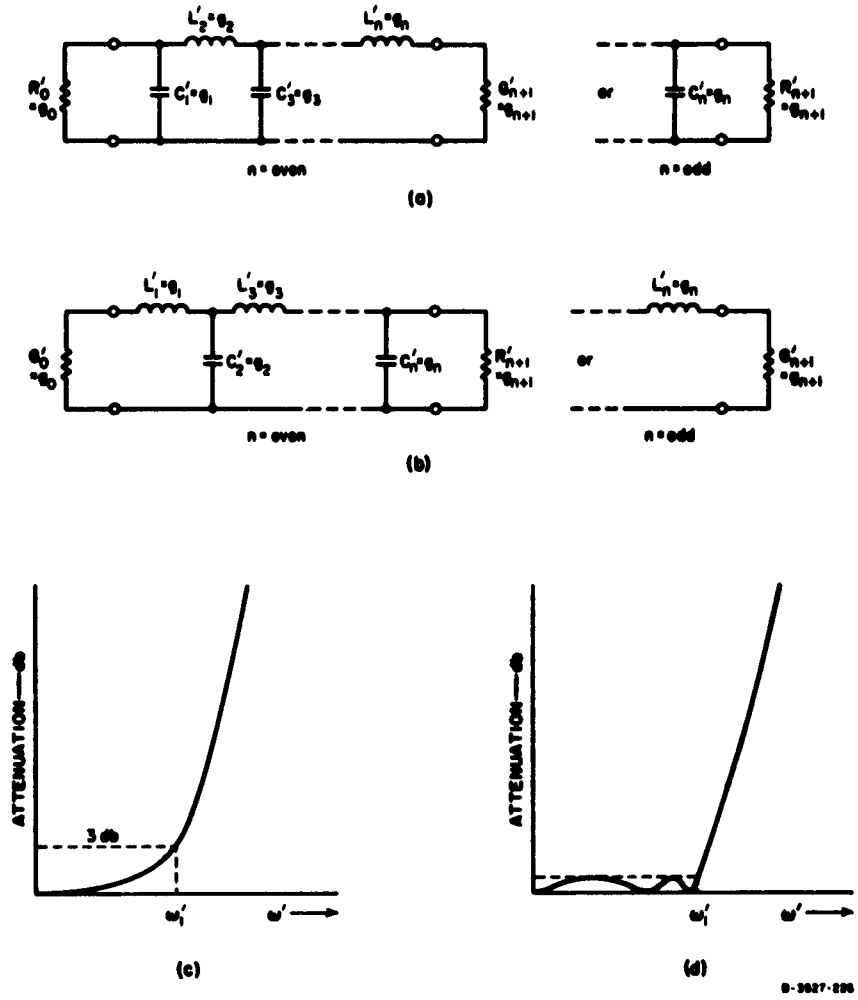

FIG. II B-1 LOW-PASS PROTOTYPE FILTER: FOUR BASIC CIRCUIT TYPES DEFINING THE PARAMETERS $g_0, g_1, \ldots, g_{n+1}$ AND MAXIMALLY FLAT AND EQUI-RIPPLE CHARACTERISTICS DEFINING THE BAND-EDGE ω_1'

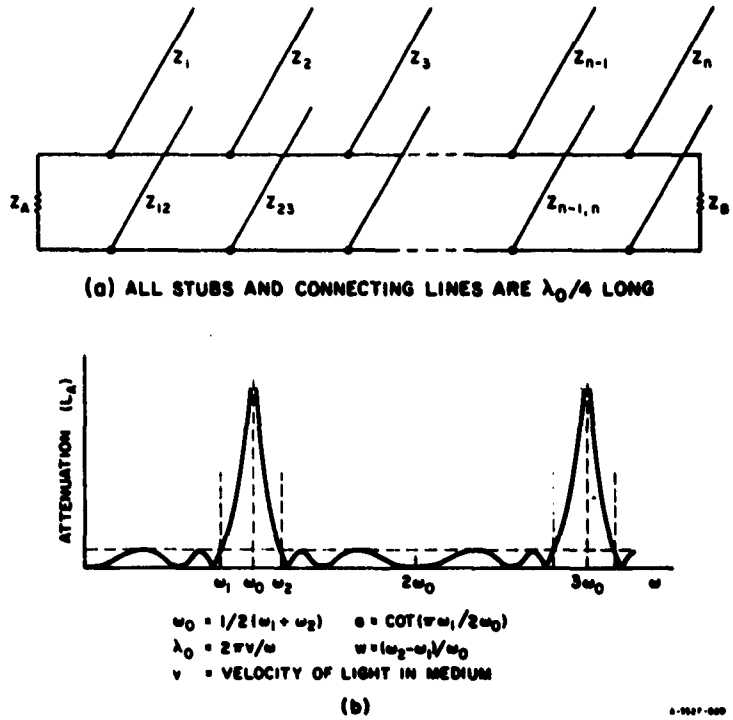

FIG. II B-2 BAND-STOP FILTER: TRANSMISSION-LINE FILTER DERIVED FROM n-ELEMENT LOW-PASS PROTOTYPE, AND EQUI-RIPPLE CHARACTERISTIC DEFINING CENTER FREQUENCY ω_0 PARAMETER a, AND STOP-BAND FRACTIONAL BANDWIDTH w

Table II B-1

DEFINITION OF PARAMETERS AND CORRESPONDENCE OF CRITICAL FREQUENCIES IN ω'-PLANE AND ω-PLANE

TRANSFORMATION	
$\omega' = \Lambda \tan\left(\frac{\pi}{2}\frac{\omega}{\omega_0}\right)$	
DEFINITION OF PARAMETERS	
ω' = Prototype frequency variable ω = Transmission line filter frequency variable $\Lambda = a\omega_1'$ $a = \cot\left(\frac{\pi}{2}\frac{\omega_1}{\omega_0}\right)$	
FREQUENCY CORRESPONDENCES	
ω'	ω
0	0
ω_1' $(0 < \omega_1' < \infty)$	$n\omega_0 \pm \omega_1$ (n even)
∞	$n\omega_0$ (n odd)

Table II B-2

EXACT EQUATIONS FOR BAND-STOP FILTERS WITH $\lambda_0/4$ SPACING BETWEEN STUBS

The filter structure is as shown in Fig. II B-2. For the dual case having short-circuited series stubs, replace all impedances in the equations below by corresponding admittances.

n = number of stubs

Z_A, Z_B = terminating impedances

Z_j (j = 1 to n) = impedances of open-circuited shunt stubs

$Z_{j-1,j}$ (j = 2 to n) = connecting line impedances

g_j = values of the elements of the low-pass prototype network as defined in Fig. II B-1

$\Lambda = \omega_1' a$ where ω_1' = low-pass prototype cutoff frequency and a = bandwidth parameter defined in Eq. (II B-1)

(In all cases the left terminating impedance Z_A is arbitrary)

Case of $n = 1$:

$$Z_1 = \frac{Z_A}{\Lambda g_0 g_1}\ ; \qquad Z_B = \frac{Z_A g_2}{g_0}$$

Case of $n = 2$:

$$Z_1 = Z_A\left(1 + \frac{1}{\Lambda g_0 g_1}\right); \qquad Z_{12} = Z_A(1 + \Lambda g_0 g_1)$$

$$Z_2 = \frac{Z_A g_0}{\Lambda g_2}\ ; \qquad Z_B = Z_A g_0 g_3$$

Case of $n = 3$:

Z_1, Z_{12} and Z_2—same formulas as case $n = 2$

$$Z_3 = \frac{Z_A g_0}{g_4}\left(1 + \frac{1}{\Lambda g_3 g_4}\right); \qquad Z_{23} = \frac{Z_A g_0}{g_4}(1 + \Lambda g_3 g_4)$$

$$Z_B = \frac{Z_A g_0}{g_4}$$

Table II B-2 *Concluded*

Case of $n = 4$:

$$Z_1 = Z_A\left(2 + \frac{1}{\Lambda_{g_0 g_1}}\right); \qquad Z_{12} = Z_A\left(\frac{1 + 2\Lambda_{g_0 g_1}}{1 + \Lambda_{g_0 g_1}}\right)$$

$$Z_2 = Z_A\left(\frac{1}{1 + \Lambda_{g_0 g_1}} + \frac{g_0}{\Lambda_{g_2}(1 + \Lambda_{g_0 g_1})^2}\right); \qquad Z_{23} = \frac{Z_A}{g_0}\left(\Lambda_{g_2} + \frac{g_0}{1 + \Lambda_{g_0 g_1}}\right)$$

$$Z_3 = \frac{Z_A}{\Lambda_{g_0 g_3}}; \qquad Z_{34} = \frac{Z_A}{g_0 g_5}(1 + \Lambda_{g_4 g_5})$$

$$Z_4 = \frac{Z_A}{g_0 g_5}\left(1 + \frac{1}{\Lambda_{g_4 g_5}}\right); \qquad Z_B = \frac{Z_A}{g_0 g_5}$$

Case of $n = 5$:

Z_1, Z_{12}, Z_2, Z_{23}, Z_3—same formulas as case $n = 4$

$$Z_4 = \frac{Z_A}{g_0}\left(\frac{1}{1 + \Lambda_{g_5 g_6}} + \frac{g_6}{\Lambda_{g_4}(1 + \Lambda_{g_4 g_5})^2}\right); \qquad Z_{34} = \frac{Z_A}{g_0}\left(\Lambda_{g_4} + \frac{g_6}{1 + \Lambda_{g_5 g_6}}\right)$$

$$Z_5 = \frac{Z_A g_6}{g_0}\left(2 + \frac{1}{\Lambda_{g_5 g_6}}\right); \qquad Z_{45} = \frac{Z_A g_6}{g_0}\left(\frac{1 + 2\Lambda_{g_5 g_6}}{1 + \Lambda_{g_5 g_6}}\right)$$

$$Z_B = \frac{Z_A g_6}{g_0}$$

To use Table II B-2, one must determine the following quantities:

(1) The left-hand terminating impedance Z_A for the shunt stub type filter, or Y_A of the series stub type filter (dual case)

(2) The element values of the prototype circuit g_j (j = 0 to n + 1) and the cutoff frequency ω_1' of the prototype

(3) The stop-band center frequency ω_0

(4) The bandwidth parameter a.

Items 1 and 3 are arbitrary, and Item 2 may be obtained from tables listed in Refs. 6 through 8, or from any suitable prototype ladder circuit consisting of alternate series inductors and shunt capacitors. The element values g_j (j = 1 to n) are the inductance of the series inductors in henries and the capacitance of the shunt capacitors in farads. The first and last elements g_0 and g_{n+1} are the prototype filter terminations given as resistance in ohms or conductance in mhos according to Fig. II B-1.

Item 4 is calculated from the formula

$$a = \cot\left(\frac{\pi}{2}\frac{\omega_1}{\omega_0}\right) \qquad \text{(II B-1)}$$

where ω_1 is the lower cutoff frequency of the transmission line filter which corresponds with ω_1' of the low-pass prototype filter.

The following example will illustrate the use of the design formulas and the practical realization of a strip-line filter employing open-circuited stubs. A band-stop filter having 50-ohm input impedance, 0.1-db pass-band ripple, and 60 percent stop-band bandwidth is desired and a three-stub design is chosen. The center of the stop band is to be 1.6 Gc. The prototype element values obtained from Table 13-1 of Ref. 8, page 202, are $g_0 = g_4 = 1$, $g_1 = g_3 = 1.0315$, and $g_2 = 1.1474$. The quantity $\Lambda = \omega_1' a$ is next computed. For the prototype chosen $\omega_1' = 1$ radian per second. From the fractional bandwidth $w = 0.6$ as defined in Fig. II B-2, we obtain $\omega_1/\omega_0 = 0.7$ and the bandwidth parameter $a = \cot(\pi\omega_1/2\omega_0)$ is found to be 0.50953, whence $\Lambda = 0.50953$. Now using $Z_A = 50$ ohms as the source impedance we calculate each stub and connecting-line impedance. Since n is odd and the prototype design is symmetrical,

the design formulas here yield a symmetrical transmission line design so that the right-hand terminating impedance Z_g = 50 ohms. The stub impedances are calculated from the design formulas of Table II B-2 for n = 3 to be $Z_1 = Z_3$ = 145.1 ohms and Z_2 = 85.5 ohms. The two connecting-line impedances are $Z_{12} = Z_{23}$ = 76.3 ohms. Each stub and connecting line is then made one-quarter wavelength long at ω_0.

A filter based on the foregoing design was fabricated in strip transmission line. With air as the dielectric, $\lambda_0/4$ is found to be 1.845 inches. The center stub was replaced by two parallel stubs of twice the impedance, *i.e.* with $Z = 2Z_2$ = 171.0 ohms, in order to minimize the junction size and thereby reduce junction effect.* The essential dimensions are given in Fig. II B-3. The stub lengths were reduced by an amount slightly more than one diameter to allow for fringing capacitance at the ends of the stubs.

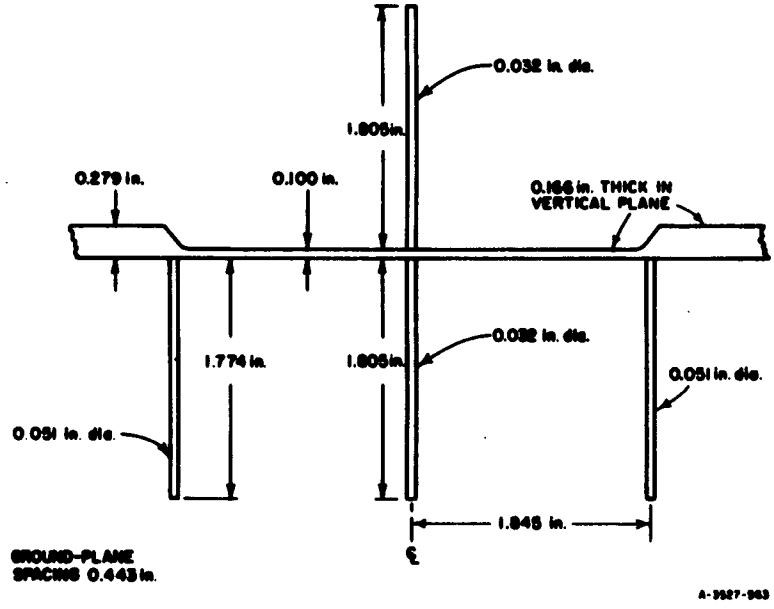

FIG. II B-3 A STRIP-LINE WIDE-STOP-BAND FILTER

* As this material is going to press some evidence has been obtained on another filter structure, which suggests that at least under some circumstances it may be unwise to replace a single stub by double stubs in parallel. Some experimental results suggest that there may be interaction between the two stubs in parallel so that regardless of their tuning they will always give two separate resonances where they are both expected to resonate at the same frequency. Also, between the two resonances the attenuation of the pair of stubs may drop very low. This possible behavior of double stubs needs further study, and is mentioned here to alert the reader of what could be a pitfall.

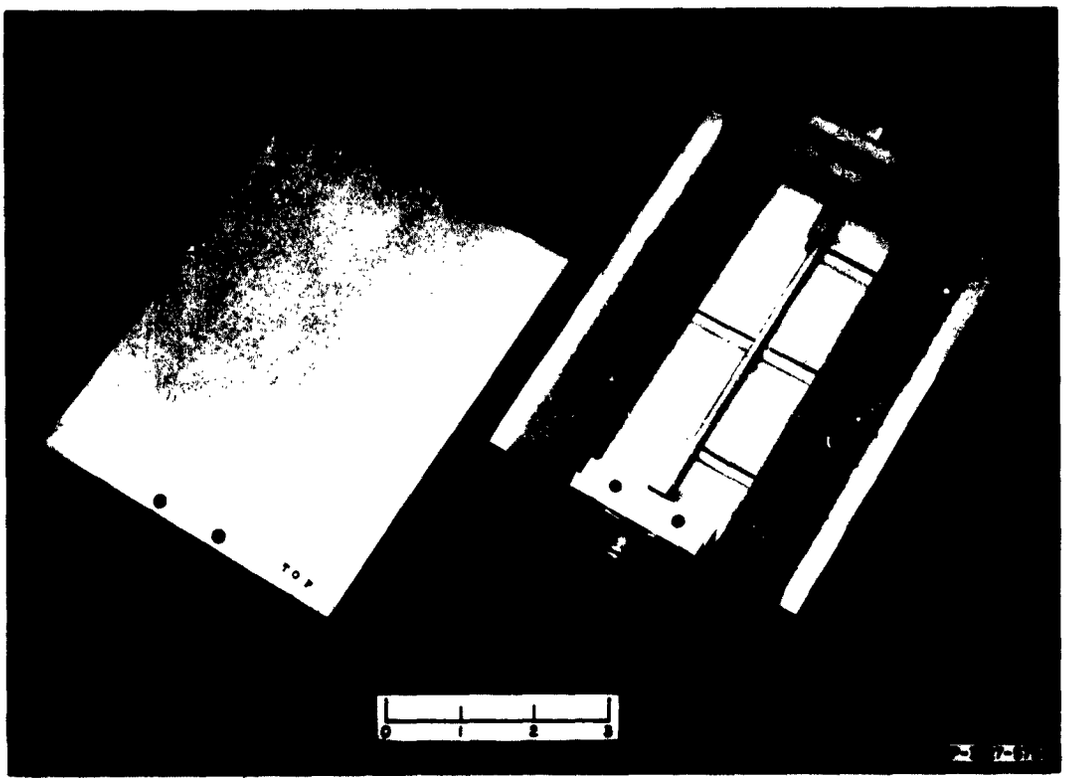

FIG. II B-4 PHOTOGRAPH OF THE STRIP-LINE WIDE-STOP-BAND FILTER

A photograph of the filter is shown in Fig. II B-4. The rectangular center-conductor dimensions were obtained from Fig. 6 of Ref. 9 and the cylindrical stubs were designed with the aid of the following approximate formula for the impedance of a round conductor between parallel planes

$$Z_0 = \frac{138}{\sqrt{\epsilon}} \log_{10} \frac{4b}{\pi d} , \qquad \text{(II B-2)}$$

where d is the diameter of center conductor and b is the plate to plate spacing. Discontinuities at impedance steps were compensated for experimentally using screws through the ground planes.

The computed and measured performance of this filter is given in Fig. II B-5. The measured results agree well with the theoretical predictions over a rather broad band; however, some improvement could have been obtained by using tuning screws to make the stubs resonate precisely at the desired stop-band center frequency.

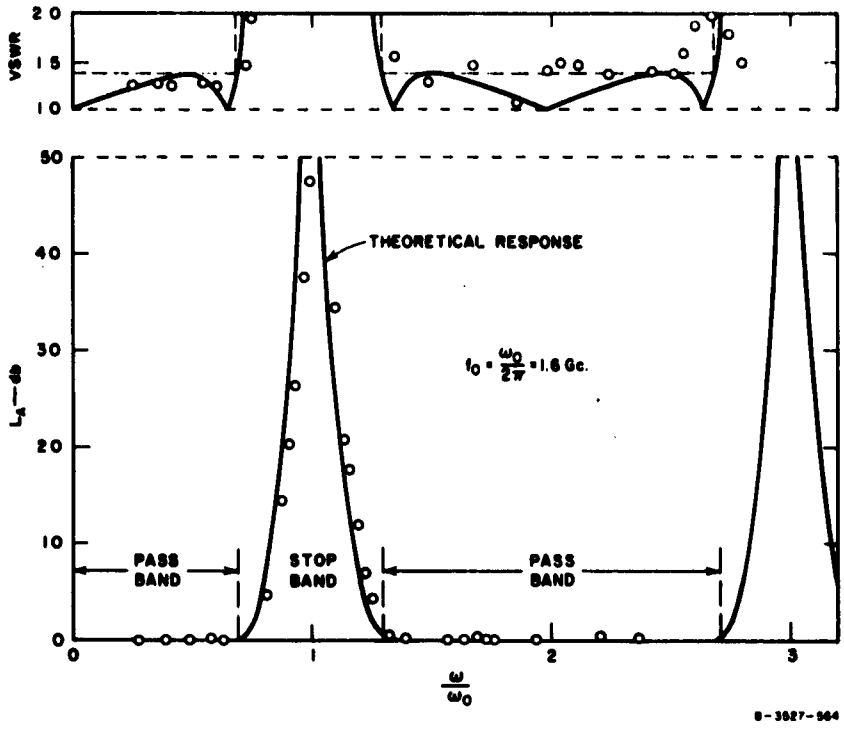

FIG. II B-5 COMPUTED AND MEASURED PERFORMANCE OF THE WIDE-STOP-BAND FILTER IN FIG. II B-3

C. MODIFICATION FOR NARROW STOP BANDS

Although the design procedure given in Part B is theoretically exact for stop bands of any width it does not produce a practical filter design for very narrow stop bands, for which shunt stub impedances of the order of 1000 ohms or more would be required in a 50-ohm system. One can, however, substitute for each open-circuited stub of length $\lambda_0/4$ a capacitively coupled short-circuited stub of electrical length $\phi_0 < \pi/2$. The connecting lines fortunately have impedances that are the same order of magnitude as the source impedance.

The coupling capacity C_j, the short-circuit stub length ϕ_0, and the impedance Z_j' are calculated from the design formulas of Fig. II C-1. The function $F(\phi)$ of the design formulas is tabulated on page 48 of Quarterly Report 3 for this project.[10] The original stub and its capacitively-coupled substitute are, by reason of the design formulas, exactly equivalent at stop-band center ω_0, and because they both present a very high impedance in shunt with the main line at other frequencies, one can expect the

modified filter and the exact design to have very nearly identical performance over the band of interest. This range of excellent performance was shown in a design example to extend from zero to at least $1.5\omega_0$. The design formulas of Fig. II C-1 permit an arbitrary choice of either Z_j', the impedance of the short-circuited stub, or C_j the gap capacitance; however, construction is simpler if all Z_j' are equal. Here the Z_j' should be approximately 75 ohms for coaxial-line or strip-line resonators in order to have high unloaded Q's, while at the same time the C_j must not be so large that the corresponding very small coupling gaps create tolerance problems. Ordinarily a filter of this type will have provision for tuning each stub resonator by means of tuning screws. A suitable strip-line design for such a filter is shown in Quarterly Report 3 for this project,[10] Fig. III-5b, page 45.

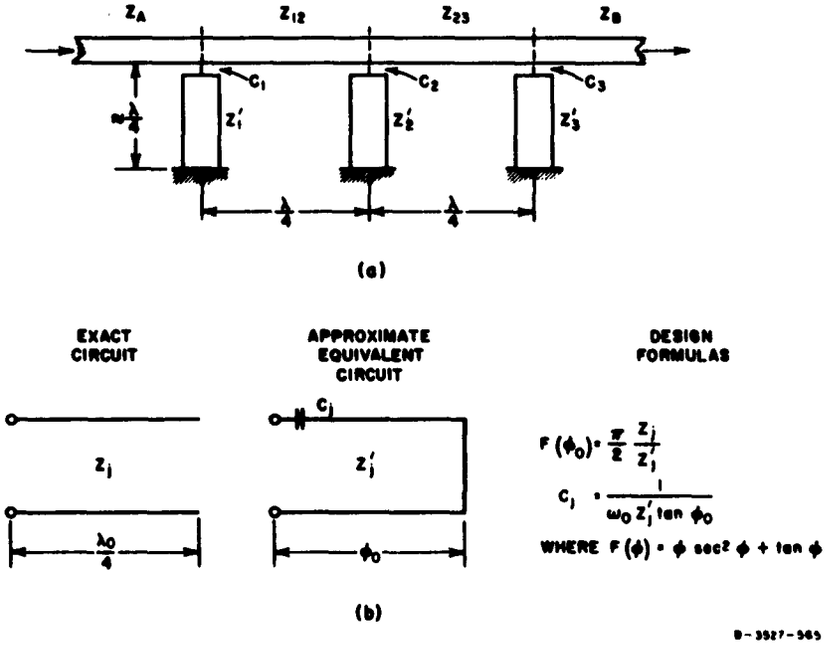

FIG. II C-1 STRIP-LINE STRUCTURE FOR BAND-STOP FILTERS WITH NARROW STOP BANDS

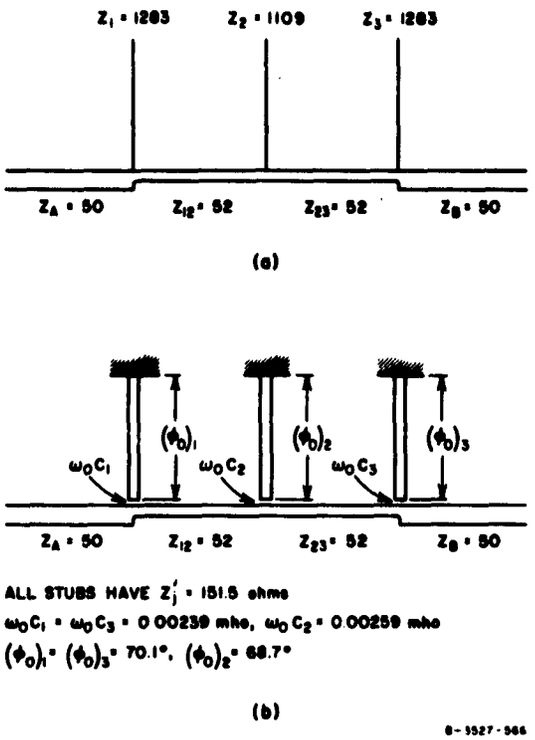

FIG. II C-2 NARROW-STOP-BAND FILTERS

A narrow-stop-band filter based on a prototype with 0.1-db Tchebyscheff ripple was designed by the above method yielding the filters of Fig. II C-2. The upper figure is the exact design and the lower figure is the derived filter using capacitively-coupled resonators. The computed response of the derived filter is shown in Figs. II C-3 and II C-4 along with that of the exact design. The response of the derived filter is seen to be very close to that of the exact design over the range $0 < \omega/\omega_0 < 1.5$, and to be a fair approximation elsewhere.

D. FORMULAS FOR FILTERS WITH $3\lambda_0/4$ SPACING BETWEEN RESONATORS

As previously mentioned, in the case of narrow-stop-band, waveguide band-stop filters, interaction effects due to the fringing fields in the vicinity of the resonator coupling irises can cause considerable disruption of the stop band when $\lambda_0/4$ spacing is used between resonators.[12] It has been found, however, that this difficulty is eliminated if $3\lambda_0/4$ spacing is used between resonators.[12]

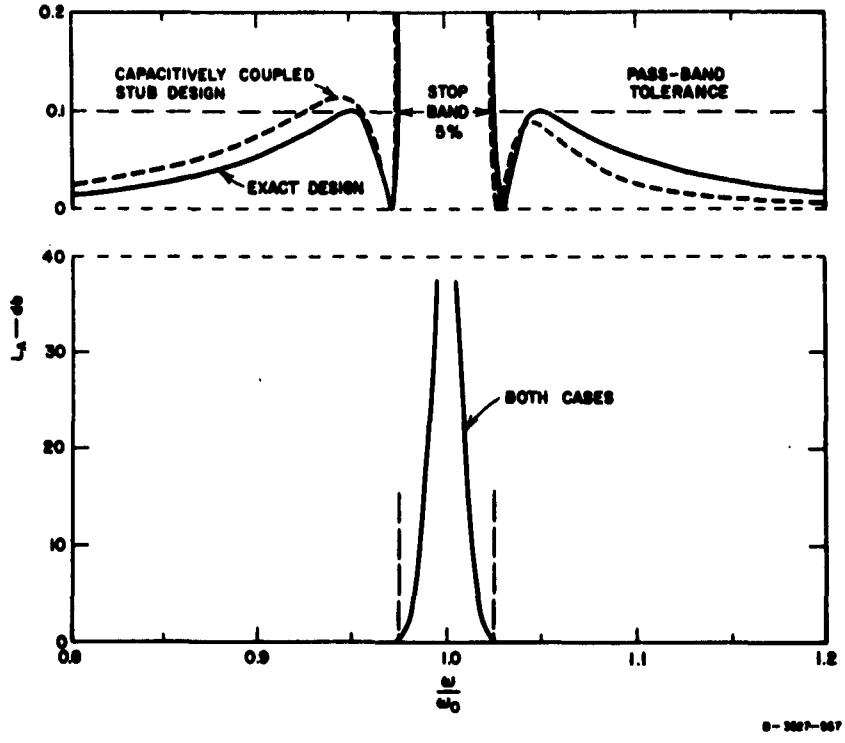

FIG. II C-3 COMPUTED RESPONSE OF THE FILTERS IN FIG. II C-2

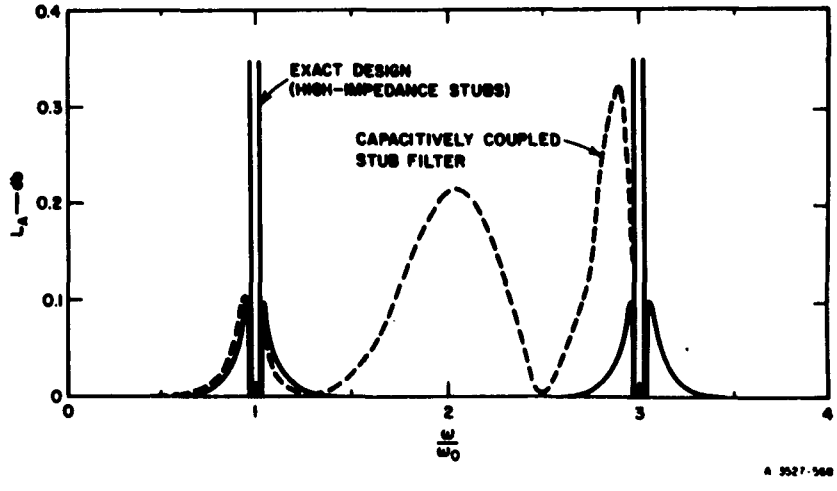

FIG. II C-4 THE RESPONSES IN FIG. II C-3 WITH AN ENLARGED SCALE

Table II D-1

EXACT EQUATIONS FOR BAND-STOP FILTERS WITH $3\lambda_0/4$ SPACING BETWEEN STUBS OR RESONATOR IRISES

The filter structure is of the form in Fig. II D-1(a). For the dual case in Fig. II D-1(b), replace all admittances in the equations below with corresponding impedances.

n = number of stubs

Y_A, Y_B = terminating admittances

Y_j (j = 1 to n) = admittances of short-circuited series stubs

$(Y_{j-1,j})_k$ = admittance of kth (k = 1, 2 or 3) connecting line from the left between stubs $j-1$ and j

g_j = values of the elements of the low-pass prototype network as defined in Fig. II B-1

$\Lambda = \omega_1'\alpha$ where ω_1' = low-pass cutoff frequency and α = bandwidth parameter defined in Eq. (II B-1)

(In all cases the left terminating impedance is arbitrary)

Case of $n = 2$:

$$Y_1 = Y_A\left(1 + \frac{1}{\Lambda g_0 g_1}\right); \qquad (Y_{12})_1 = Y_A(1 + \Lambda g_0 g_1)$$

$$Y_2 = Y_A\frac{g_0}{\Lambda g_2}(1 + 2\Lambda g_2 g_3); \qquad (Y_{12})_2 = Y_A g_0 g_3\left(\frac{1}{1 + \Lambda g_2 g_3}\right)$$

$$Y_B = Y_A g_0 g_3; \qquad (Y_{12})_3 = Y_A g_0 g_3\left(\frac{1 + 2\Lambda g_2 g_3}{1 + \Lambda g_2 g_3}\right)$$

Case of $n = 3$:

$$Y_1 = Y_A\left(3 + \frac{1}{\Lambda g_0 g_1}\right) \qquad (Y_{12})_1 = Y_A\left(\frac{1 + 3\Lambda g_0 g_1}{1 + 2\Lambda g_0 g_1}\right)$$

$$(Y_{12})_2 = Y_A\left(\frac{1 + \Lambda g_0 g_1}{1 + 2\Lambda g_0 g_1}\right)$$

$$Y_2 = Y_A\frac{g_0}{\Lambda g_2} \qquad (Y_{12})_3 = Y_A(1 + \Lambda g_0 g_1)$$

$$(Y_{23})_1 = Y_A\frac{g_0}{g_4}(1 + \Lambda g_3 g_4)$$

$$Y_3 = Y_A\frac{g_0}{g_4}\left(3 + \frac{1}{\Lambda g_3 g_4}\right) \qquad (Y_{23})_2 = Y_A\frac{g_0}{g_4}\left(\frac{1 + \Lambda g_3 g_4}{1 + 2\Lambda g_3 g_4}\right)$$

$$Y_B = Y_A\frac{g_0}{g_4} \qquad (Y_{23})_3 = Y_A\frac{g_0}{g_4}\left(\frac{1 + 3\Lambda g_3 g_4}{1 + 2\Lambda g_3 g_4}\right)$$

Table II D-1 presents equations for the design of filters with series-connected stubs with $3\lambda_0/4$ spacings between stubs, for the cases of $n = 2$ and $n = 3$ stubs. The configuration under consideration is shown in Fig. II D-1(a); however, by duality, the same equations can be made to apply also to the structure in Fig. II D-1(b) by simply redefining all of the admittances in Table II D-1 as impedances. The resonator susceptance slope parameters for the series stubs in Fig. II D-1(a) are given by

$$b_j = \frac{\pi}{4} Y_j \quad . \qquad \text{(II D-1)}$$

Having the admittances of the connecting line sections, and also the slope parameters required for the various resonators, the designer can carry out the remainder of the waveguide filter design using the procedure that was discussed previously.[10,12]

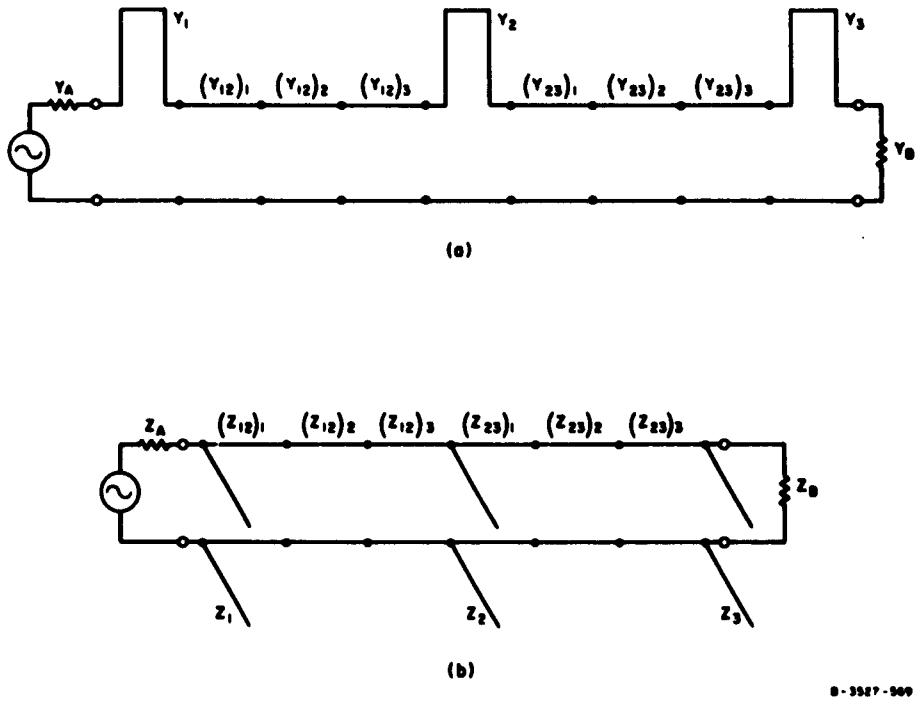

FIG. II D-1 BAND-STOP FILTERS WITH 3 $\lambda_0/4$ SPACING BETWEEN $\lambda_0/4$ STUBS

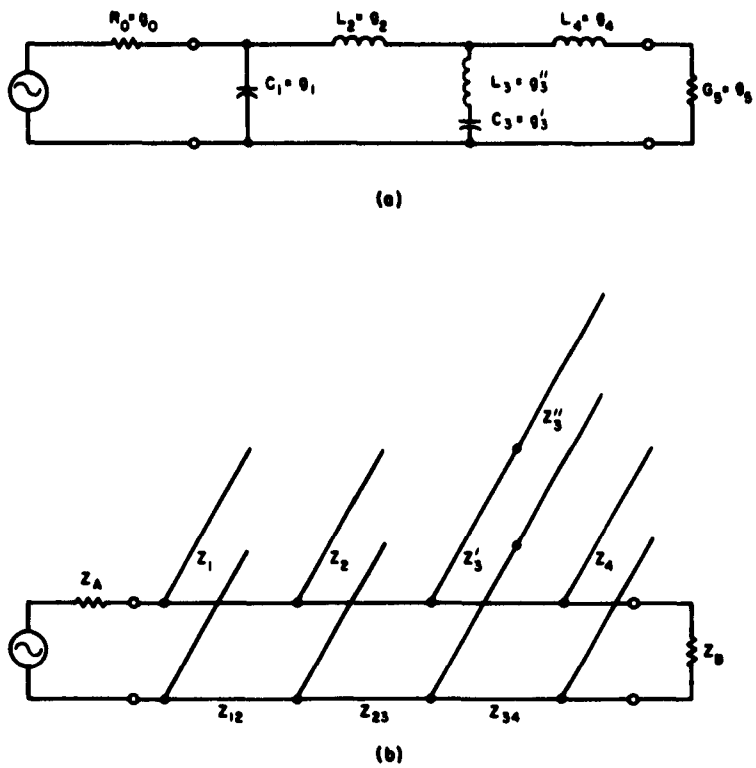

USE DESIGN FORMULAS IN TABLE II B-2 FOR CASE OF $n=4$, EXCEPT IN PLACE OF Z_3 SUBSTITUTE:

$$Z_3' = \frac{Z_A}{g_0}\left(A g_3'' + \frac{1}{A g_3'}\right) \quad , \quad Z_3'' = \frac{Z_A}{A g_0 g_3'}\left[1 + \frac{1}{A^2 g_3' g_3''}\right]$$

A-3527-570

FIG. II E-1 LOW-PASS PROTOTYPE AND BAND-STOP FILTER WITH EQUI-RIPPLE PASS BANDS AND STOP BANDS

E. FILTERS WITH EQUAL-RIPPLE PASS-BAND AND STOP-BAND ATTENUATION

The filters described heretofore have all their poles of attenuation at the design frequency ω_0 (and at odd multiples thereof) with the result that the stop band is relatively narrow for high values of attenuation. For example, the computed filter response of Fig. II B-5 has a 60-percent stop band for 0.1-db attenuation while the 45-db stop band is 10 percent of center frequency. We desire a method, therefore, of spreading the attenuation poles in the stop band to achieve sharper cutoffs and broader regions of high attenuation without affecting the pass-band response adversely. This can be done by employing a low-pass prototype that has just one pole of attenuation at a finite frequency and that has Tchebyscheff ripple in both pass- and stop bands.[11] It can be shown that more than one finite frequency pole in the low-pass prototype would disrupt the design procedure discussed herein. A schematic diagram of a prototype filter ($n = 4$) with one pole of attenuation at a finite frequency is shown in Fig. II E-1(a), and Fig. II E-1(b) shows its corresponding transmission-line filter together with design formulas, which supplement those in Table II B-2. Tables of element values for filters of the type shown in Fig. II E-1(a) yielding the response shape of Fig. II E-2(a) have been published by the Telefunken company[11] and can be used with the design formulas of Fig. II E-1 and Table II B-2, provided that the following change of notation is made on the element values in the Telefunken tables:[11] The element values (L_1, L_2,C_2,L_3,C_4) as given in the Telefunken tables are to be reversed in position (C_4,L_3,C_2,L_2,L_1) and then given the standard notation used herein (g_1,g_2,g_3', g_3'',g_4) respectively. Also, for this case, $g_0 = g_5 = 1$ for the symmetrical filter, and $g_0 = 1/(\text{right-hand terminating resistance})$ and $g_5 = 1$ for the asymmetrical filter. The two-terminal

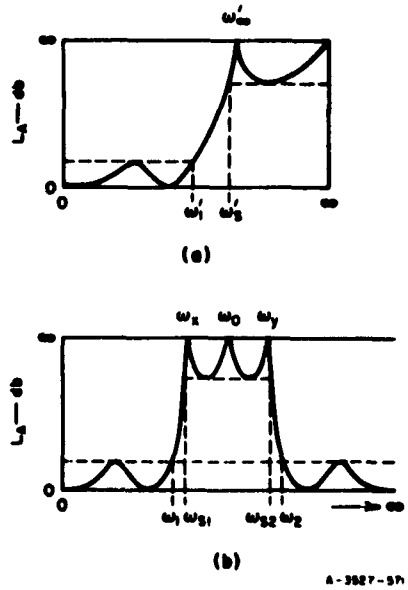

FIG. II E-2 RESPONSE OF FILTER NETWORKS OF FIG. II E-1
(a) LOW-PASS PROTOTYPE
(b) TRANSMISSION-LINE FILTER

circuit consisting of capacitor C_2 and inductor L_2 in series has for its exact transform the series-connected open-circuited and short-circuited stubs as shown in Fig. II E-3(b). Such a network cannot be easily realized, however, and the exactly equivalent two-section tandem network shown just below the former is sometimes preferable. Although the above methods for realizing the susceptance B in Fig. II E-3(b) are exact, they may yield extremes of impedance values in the two-stub section. To get around such difficulties, the approximate equivalent network of two unequal length stubs in parallel as shown in Fig. II E-3(c) may be used in place of the exact design. The shunt susceptance of the substitute

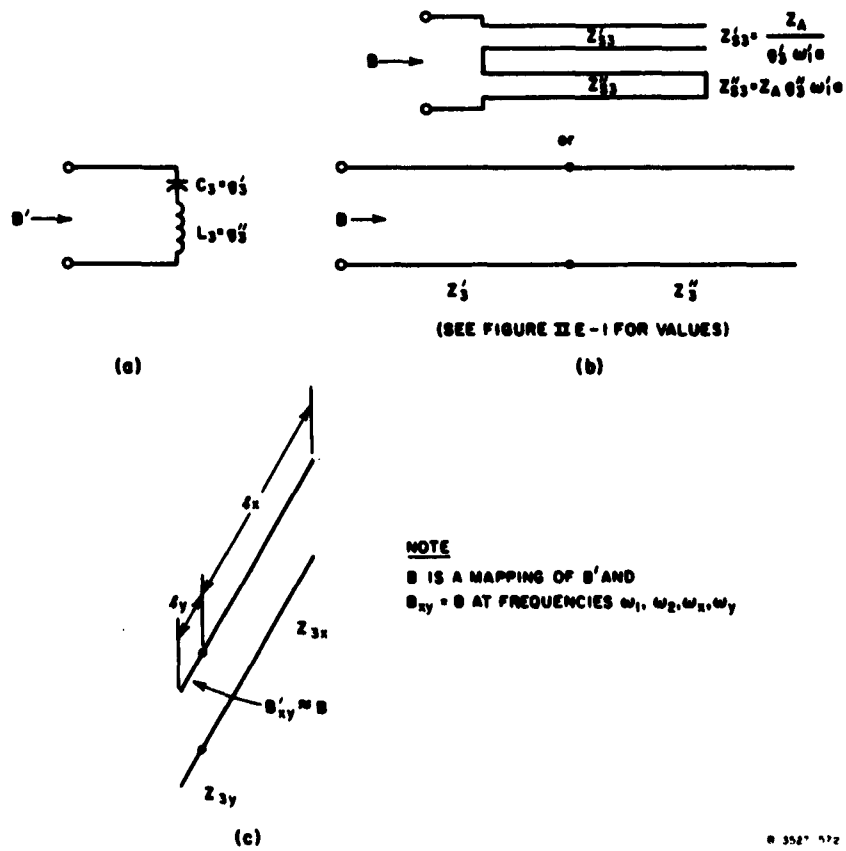

FIG. II E-3 TWO-TERMINAL SHUNT NETWORK YIELDING POLES OF ATTENUATION NEAR STOP-BAND EDGE

stubs Z_{3x} and Z_{3y} in parallel is exactly equal to that of the two-section exact-design stubs Z_3' and Z_3'' at frequencies ω_1, ω_2, ω_x and ω_y. The design formulas for Z_{3x} and Z_{3y} are

$$Z_{3y} = \left[X_3|_{\omega_1}\right]\left[\frac{\tan\theta_{y2}\tan\theta_{x1} - \tan\theta_{y1}\tan\theta_{x2}}{\tan\theta_{x1} + \tan\theta_{x2}}\right] \qquad \text{(II E-1)}$$

and

$$Z_{3x} = \left[X_3|_{\omega_1}\right]\left[\frac{\tan\theta_{y1}\tan\theta_{x2} - \tan\theta_{y2}\tan\theta_{x1}}{\tan\theta_{y1} + \tan\theta_{y2}}\right] \qquad \text{(II E-2)}$$

where

$$X_3|_{\omega_1} = \frac{Z_A}{g_0}\left[\omega_1' g_3'' - \frac{1}{\omega_1' g_3'}\right] \qquad \text{(II E-3)}$$

$$\theta_{uv} = \frac{\pi}{2}\frac{\omega_v}{\omega_u} \quad \text{radians},$$

and the frequency subscripts 1, 2, x, and y are defined in Fig. II E-2. The lengths l_x and l_y of the stubs of impedance Z_{3x} and Z_{3y}, respectively, are calculated from the relationship

$$\omega_x l_x = \omega_y l_y = \frac{\pi v}{2} \qquad \text{(II E-4)}$$

where v = velocity of light in medium.

The main features of this approximate type of design are shown in the filter of Fig. II E-4. The response of this filter is given in Fig. II E-5. Although the exact-design filter response is not given in Fig. II E-5, the comparative performance of the two types can be inferred from the dashed lines which form the bounds of the equi-ripple exact response. It is apparent that over a frequency range from zero to almost $2\omega_0$ (twice stop-band center frequency) the approximate design filter response is remarkably close to the ideal response boundaries, and although there is deviation from the ideal above that region the filter is still useful. The advantage gained is the reduction of the range of

impedances in the filter from a ratio of 12 to 1 to about 4.5 to 1. The prototype element values for this filter are $g_0 = 1$, $g_1 = 0.9304$, $g_2 = 1.373$, $g_3' = 1.278$, $g_3'' = 0.1017$, $g_4 = 0.8357$, and $g_5 = 1$ as given on page 50, line 27 of the Telefunken tables[11] (but in reverse order as explained above). The maximum pass-band reflection coefficient is 15 percent (0.1-db attenuation), and the minimum stop-band attenuation is 45.2 db. The pole of attenuation in the stop band of the prototype occurs at $\omega_s' = 2.773\omega_1' = 2.77$, since $\omega_1' = 1$. The edge of the prototype stop band for 45.2-db attenuation is at $\omega_s' = 2.539$. In the transmission-line filter (exact design) the 0.1-db stop-band edges are $0.5\omega_0$ and $1.5\omega_0$ (100 percent bandwidth) and the 45.2-db bandwidth extends from $\omega_{s1} = 0.761$ to $\omega_{s2} = 1.239$ (48 percent bandwidth). The normalized transmission-line impedances for the exact design are $Z_A = 1$, $Z_1 = 3.075$, $Z_2 = 0.714$, $Z_3' = 0.8842$, $Z_3'' = 8.549$, $Z_4 = 2.197$, $Z_B = 1$ and $Z_{12} = 1.482$, $Z_{23} = 1.891$, $Z_{34} = 1.836$. For the approximate design, we have in place of the two-section stub with impedances $Z_3' = 0.8842$ and $Z_3'' = 8.549$, two shunt stubs of impedance $Z_{3x} = 1.470$ and $Z_{3y} = 1.915$. The electrical lengths of these stubs at stop-band center frequency are $\theta_{y0} = 1.287$ radians and $\theta_{x0} = 2.015$ radians. The design parameter $\Lambda = \alpha\omega_1' = 1$.

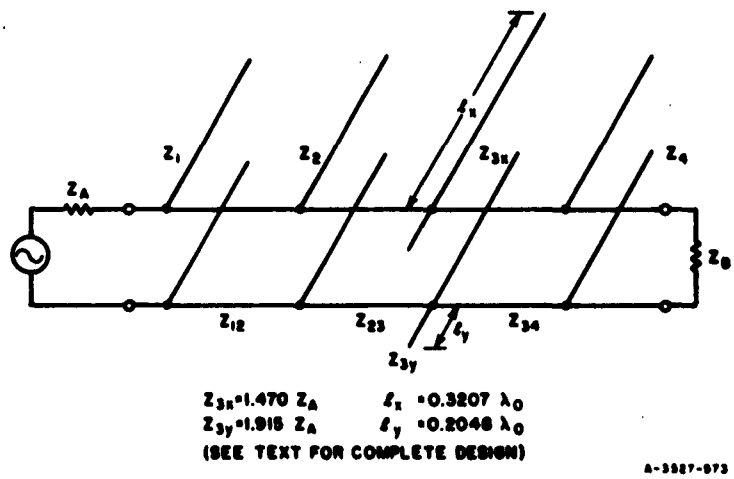

FIG. II E-4 PRACTICAL ADAPTATION OF EXACT DESIGN FOR TCHEBYSCHEFF RESPONSE IN PASS BAND AND STOP BAND (n = 4)

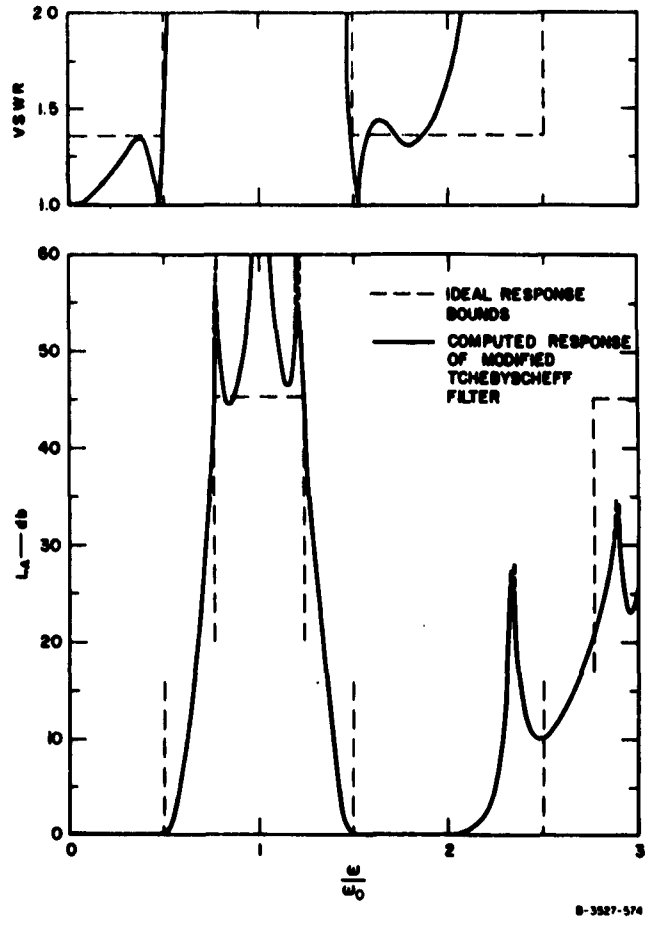

FIG. II E-5 COMPUTED RESPONSE OF FILTER OF FIG. II E-4

Although the specific example used here to illustrate the design method yielded reasonable values of impedance this will not necessarily be true for all filter specifications. For filters with narrow stop- or pass bands, the filter designer may have to accept less discrimination between the pass band and the stop band than he can demand when the pass- and stop bands are approximately equal in width in order to obtain reasonable values for the stub transmission-line impedances.

F. DERIVATION OF THE DESIGN EQUATIONS IN THIS SECTION

The design procedure of this section hinges on Kuroda's identity.[2,4] This identity is realized in transmission line as shown in Fig. II F-1. Note that this identity says that a circuit consisting of an open-circuited shunt stub and a connecting line of the same length has an exact equivalent circuit consisting of a short-circuited series stub with a connecting line at the opposite side.

Figure II F-2 traces out how Kuroda's identity is used to relate a band-stop filter of the type in Fig. II B-2(a) to a low-pass prototype filter. Figure II F-2(a) shows a low-pass prototype filter for the case

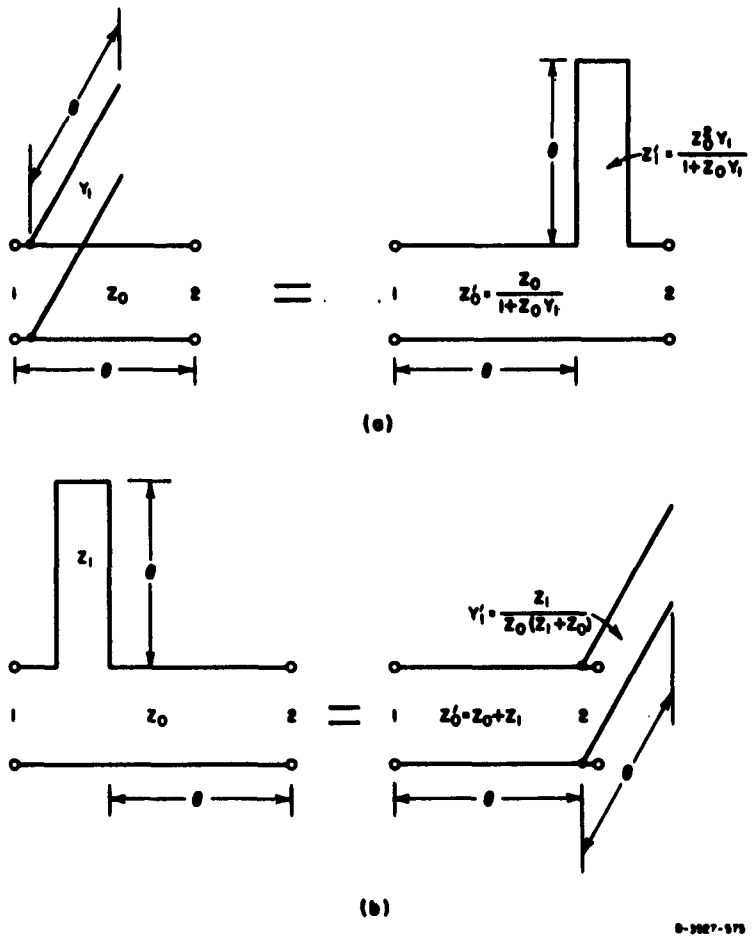

FIG. II F-1 KURODA'S IDENTITY IN TRANSMISSION-LINE FORM

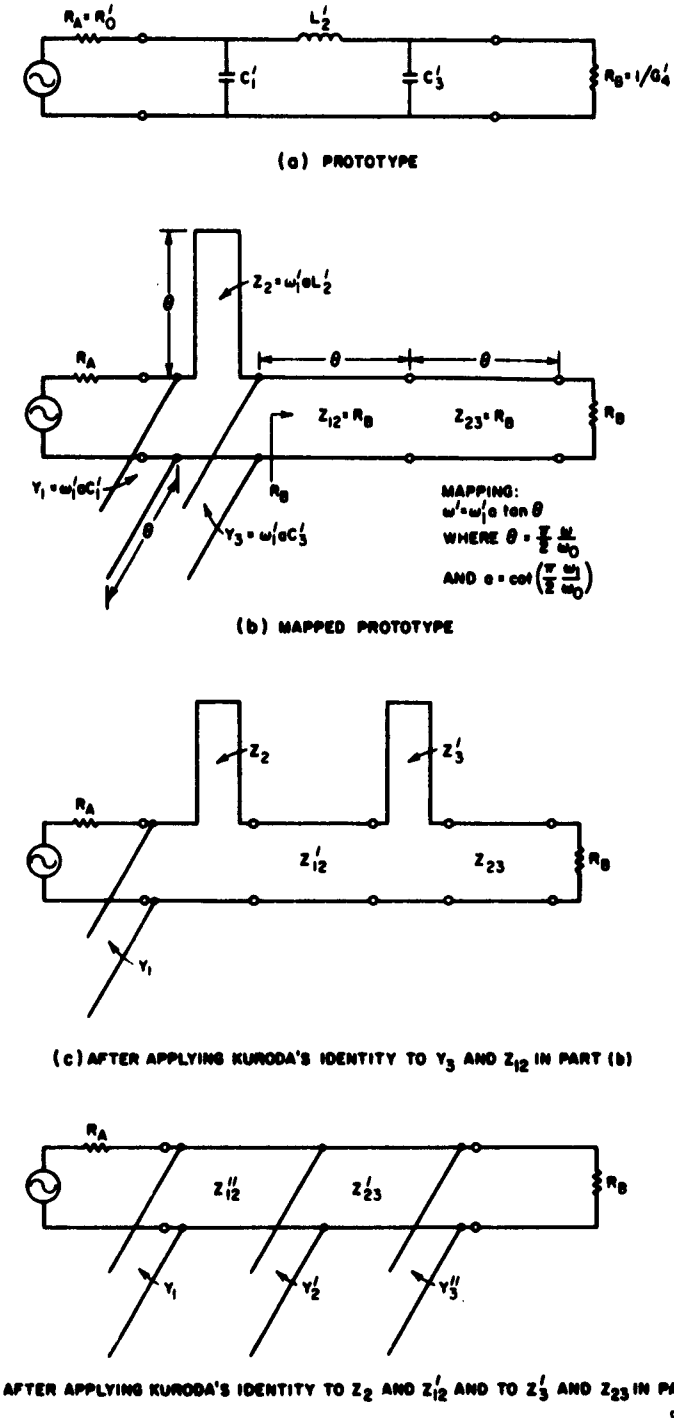

FIG. II F-2 STAGES IN THE TRANSFORMATION OF A LOW-PASS PROTOTYPE FILTER INTO A BAND-STOP TRANSMISSION-LINE FILTER

of $n = 3$ reactive elements. Applying the mapping equation of Table II B-1 to the shunt susceptances and series reactances of this filter gives

$$\omega' C_j' = C_j' \omega_1' a \tan\left(\frac{\pi}{2}\frac{\omega}{\omega_0}\right) \qquad \text{(II F-1)}$$

$$\omega' L_j' = L_j' \omega_1' a \tan\left(\frac{\pi}{2}\frac{\omega}{\omega_0}\right) \quad . \qquad \text{(II F-2)}$$

Note that the right side of Eq. (II F-1) corresponds to the susceptance of an open-circuited stub having a characteristic admittance

$$Y_j = C_j' \omega_1' a \quad , \qquad \text{(II F-3)}$$

the stub being $\lambda_0/4$ long at ω_0. Similarly, the right side of Eq. (II F-2) corresponds to the reactance of a short-circuited stub of characteristic impedance

$$Z_j = L_j' \omega_1' a \qquad \text{(II F-3)}$$

when the stub is $\lambda_0/4$ long at frequency ω_0. Thus, the shunt capacitors in the low-pass prototype become open-circuited shunt stubs in the mapped filter, while the series inductance in the prototype becomes a short-circuited series stub in the mapped filter.

Note that in the mapped filter in Fig. II F-2(b), the terminations seen by the reactive part of the filter are still R_A on the left and R_B on the right. However, on the right two line sections of impedance $Z_{12} = Z_{23} = R_B$ have been added. Since their characteristic impedance matches that of the termination, they do not affect the attenuation characteristic of the circuit; their only effect on the response is to give some added phase shift. The circuit in Fig. II F-2(b) then has a response which is the desired exact mapping of the low-pass prototype response. The only trouble with the filter in Fig. II F-2(b) is that it contains a series stub which is difficult to construct in a shielded TEM-mode microwave structure.

The series stub in Fig. II F-2(b) can be eliminated by application of Kuroda's identity (Fig. II F-1). Applying Kuroda's identity to stub Y_3 and line Z_{12} in Fig. II F-2(b) gives the circuit in Fig. II F-2(c).

Then applying Kuroda's identity simultaneously to stub Z_2 and line Z'_{12} and stub Z'_3 and line Z_{23} in Fig. II F-2(c) gives the circuit in Fig. II F-2(d). Note that the circuit in Fig. II F-2(d) has exactly the same input impedance and over-all transmission properties as the circuit in Fig. II F-2(b), while the circuit in Fig. II F-2(d) has no series stubs.

The equations in Tables II B-2 and II D-1 were derived by use of repeated applications of the procedures described above. For reasons of convenience, the equations in the tables use a somewhat different notation than does the example in Fig. II F-2; however, the principles used are the same. The equations in Tables II B-2 and II D-1 also provide for a shift in impedance level from that of the low-pass prototype.

The slightly more complicated filter network of Part E, in which the attenuation poles are spread out in the stop band, is solved in a manner very similar to that described above. That is, each lumped element is transformed to a transmission-line section and Kuroda's identity is used to separate the stubs while causing all stubs (except for those in Branch 3) to be of one kind only as shown in Fig. II E-1. There are, however, two important differences worth further discussion. First, the series *L-C* network in Branch 3 of the low-pass prototype [Fig. III E-1(a)] requires special treatment in the process of being transformed to transmission-line stubs as described in Part E, and second, Kuroda's transformation cannot be applied to the corresponding two-stub branch of the filter. Because of this inapplicability, only one such two-stub branch is allowed in the transmission-line filter. With only one such two-stub network in the filter circuit, it is possible to insert as many quarter-wave sections as are required starting at each end and working toward the two-stub branch. This is no handicap and was in fact the method used in deriving the design equation of Tables II B-2 and II D-1.

REFERENCES

1. Richards, P. I., "Resistor-Transmission-Line Circuits," *Proc. of the IRE*, 36, pp. 217-220 (February 1948).

2. Ozaki, H., and Ishii, J., "Synthesis of Transmission-Line Networks and the Design of UHF Filters," *IRE Trans. on Circuit Theory*, CT-2, pp. 325-336 (December 1955).

3. Jones. E. M. T., "Synthesis of Wide-Band Microwave Filters to have Prescribed Insertion Loss," *IRE Convention Record*, 1956 National Convention, Part 5, pp. 119-128.

4. Ozaki, H., and Ishii, Jr., "Synthesis of a Class of Strip-Line Filters," *IRE Trans. on Circuit Theory*, CT-5, pp. 104-109 (June 1958).

5. A. I. Grayzel, "A Synthesis Procedure for Transmission Line Networks," *IRE Trans. on Circuit Theory*, CT-5, pp. 172-181 (September 1958).

6. L. Weinberg, "Network Design by Use of Modern Synthesis Techniques and Tables," Tech. Memo 427, Hughes Aircraft Company, Research Laboratories, Culver City, California (April 1956); also *Proceedings of the National Electronics Conference*, 12 (1956).

7. L. Weinberg, "Additional Tables for Design of Optimum Ladder Networks," *Journal of the Franklin Institute*, 264, Nos. 1 and 2 (July and August 1957).

8. G. L. Matthaei, *et al.*, "Design Criteria for Microwave Filters and Coupling Structures," Final Report, SRI Project 2326, Contract DA 36-039 SC-74862, Stanford Research Institute, Menlo Park, California (June 1957).

9. R. H. Bates, "The Characteristic Impedance of Shielded Slab Lines," *IRE Trans. PGMTT*-4, p. 32 (January 1956).

10. P. S. Carter, Jr., Leo Young, *et al.*, "Microwave Filters and Coupling Structures," Quarterly Progress Report No. 3, Section III, SRI Project 3527, Contract DA 36-039 SC-87398, Stanford Research Institute, Menlo Park, California (October 1961).

11. R. Saal, *Der Entwurf von Filtern mit Hilfe des Kataloges normierter Tiefpässe*, Telefunken, G.M.B.H., Backnang/Württemburg, Western Germany (1961) [Part of these tables are contained in the paper: R. Saal and E. Ulbrich "On the Design of Filters by Synthesis," *IRE Trans. PGCT*-5, pp. 284-327 (December 1958)].

12. Leo Young and G. L. Matthaei, "Microwave Filters and Coupling Structures," Quarterly Progress Report 4, SRI Project 3527, Contract DA 36-039 SC-87398, Stanford Research Institute, Menlo Park, California

III MAGNETICALLY TUNABLE FILTERS

A. GENERAL

In this section a review of the procedure employed in the establishment of the parameters and dimensions of magnetically tunable filters is given. Charts and graphs are presented which enable a designer to arrive at the dimensions of the circuit elements, including the ferrimagnetic resonators, in order to give a specified band-pass frequency response. Circuit structures are presented which appear, or which have proved to be very promising for practical applications. Two typical examples are given of the design of two-resonator band-pass filters, one of which employs a waveguide and the other a strip-transmission-line coupling circuit. Finally, the performances of two side-wall-coupled strip-transmission-line filters, one containing two resonators and the other three, are discussed. The results are compared with a previous version of the two-resonator side-wall-coupled filter and with a previously developed overlapping line version.

B. DESIGN OF RECIPROCAL MAGNETICALLY TUNABLE MICROWAVE FILTERS

An equivalent circuit composed of lumped elements, including gyrators, can be developed to represent coupled ferrimagnetic resonators. A series of ferrimagnetic resonators shown in Fig. III B-1 is coupled through the interaction of the RF magnetic dipole moments of the resonators. Whether or not a gyrator is present in the equivalent circuit representation depends on the way in which the resonators are coupled to each other and upon the way the end resonators are coupled to the input and output lines or waveguides. If the input and output coupling loops in Fig. III B-1 were orthogonal, then the equivalent circuit would contain a gyrator. If the two loops lie in the same plane as shown, then no gyrator will be present in the equivalent circuit.

The presence or absence of a gyrator in the equivalent circuit representation of multiple-coupled-ferrimagnetic-resonator filters does not affect their transfer characteristics in the cases to be considered

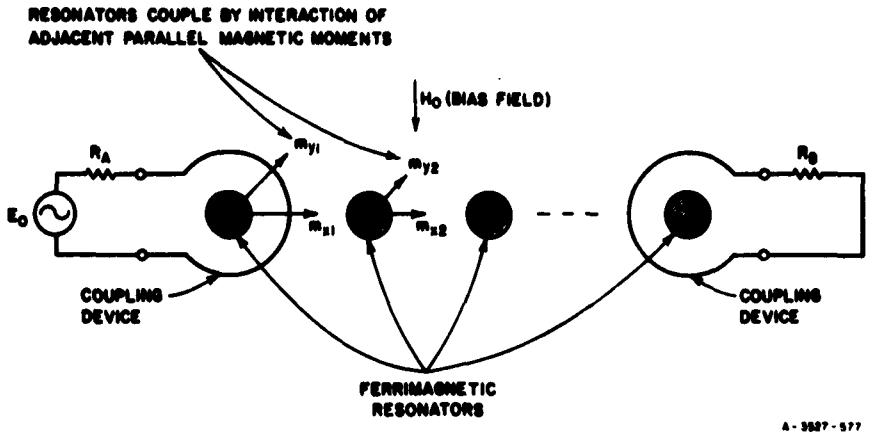

FIG. III B-1 MAGNETIC MOMENTS IN A FILTER EMPLOYING MULTIPLE FERRIMAGNETIC RESONATORS

here. Devices that employ the nonreciprocal characteristics of the ferrimagnetic resonator, such as the magnetically tunable nonreciprocal waveguide filter[1*] must be represented by circuits that contain both gyrators and resonant circuits. Some equivalent circuits for these nonreciprocal configurations in waveguide structures have been given by Patel[1] and Anderson.[2]

Figure III B-2 gives a lumped-element circuit representation of the multiple-ferrimagnetic-resonator band-pass filter. From this representation,

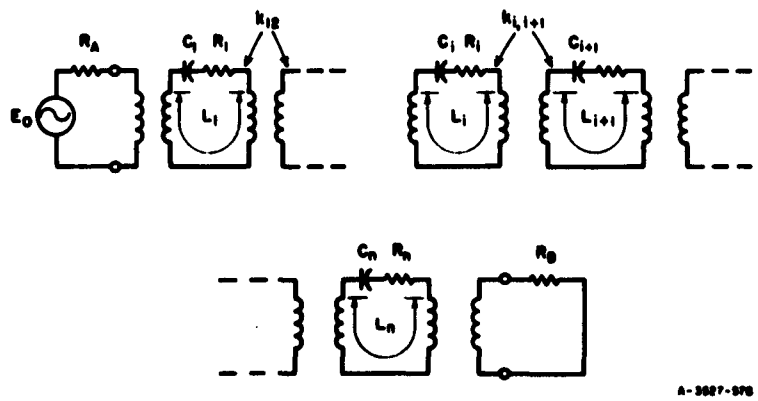

FIG. III B-2 EQUIVALENT CIRCUIT OF COUPLED FERRIMAGNETIC RESONATOR FILTER

* References are listed at the end of this section.

a systematic design procedure is carried out as follows, making use of a low-pass prototype approach to the derivation of the lumped-element band-pass circuit parameters:[3,4]

$$(Q_e)_A = \frac{\omega_1' g_1 g_0}{w} \qquad \text{(III B-1)}$$

$$(Q_e)_B = \frac{\omega_1' g_n g_{n+1}}{w} \qquad \text{(III B-2)}$$

$$k_{i,i+1} = \frac{w}{\omega_1' \sqrt{g_i g_{i+1}}} \qquad \text{(III B-3)}$$

where

$(Q_e)_A$, $(Q_e)_B$ = External Q's of input and output resonators

$k_{i,i+1}$ = Coupling coefficient between resonators

$g_0, g_1, \ldots, g_n, g_{n+1}$ = Normalized low-pass prototype element values for desired response shape (see Fig. III B-3)

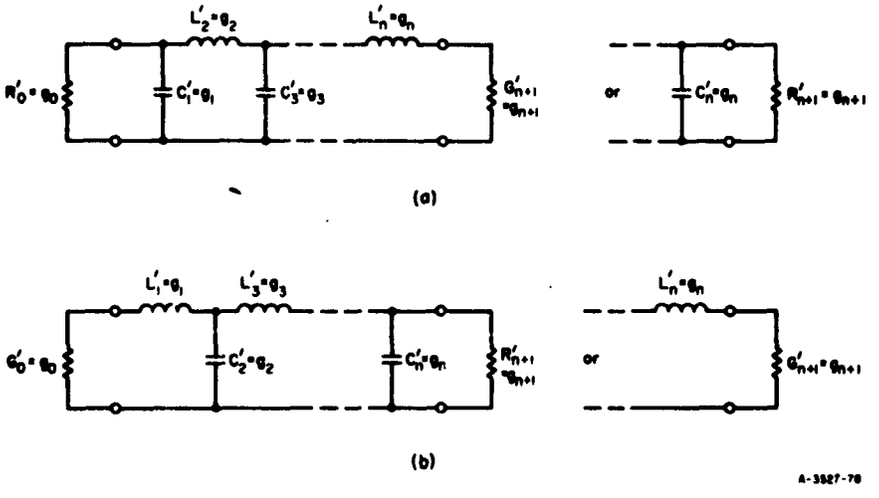

FIG. III B-3 DEFINITION OF PROTOTYPE FILTER PARAMETERS $g_0, g_1, g_2, \cdots, g_{n+1}$
A prototype circuit is shown at (a) and its dual is shown at (b). Either form will give the same response. An additional prototype parameter, ω_1', is defined in Fig. III B-4.

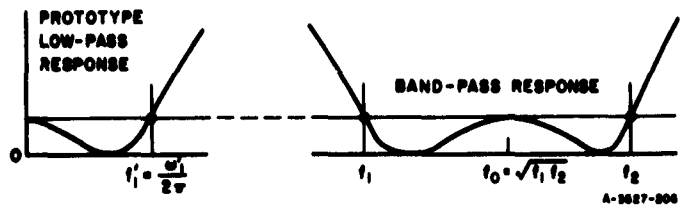

FIG. III B-4 DEFINITION OF LOW-PASS PROTOTYPE AND BAND-PASS RESPONSE FREQUENCIES

ω_1' = Cutoff frequency (radians/sec) of normalized low-pass prototype (see Fig. III B-4)

$w = (f_2 - f_1)/f_0$ = Fractional bandwidth, where f_1 and f_2 are defined in Fig. III B-4 and $f_0 = \sqrt{f_1 f_2}$.

The center-frequency dissipation loss, L_d, (*i.e.*, not including reflection loss) is given approximately by[5]

$$L_d = 4.343 \frac{\omega_1'}{w} \sum_{i=1}^{n} \left(\frac{g_i}{Q_{ui}} \right) \quad \text{db} \quad . \qquad \text{(III B-4)}$$

Here the prototype element values are assumed to be normalized so that $g_0 = 1$, and the Q_{ui} are the unloaded Q's of the resonators.

C. RESONATOR MATERIALS AND THEIR PROPERTIES

1. *General*—Several different single-crystal materials are known to have possible application in magnetically tunable filter design:

(1) Yttrium-iron-garnet (YIG)
(2) Gallium-substituted yttrium-iron-garnet (Ga-YIG)
(3) Lithium ferrite
(4) Barium ferrite.

Of these four materials, the first three now appear to be the most promising for tunable band-pass and band-reject filter applications since they have the narrowest linewidth. The properties including the unloaded $Q(Q_u)$ of YIG have been discussed in several of our previous publications[6,7] and in the literature. The remaining three resonator materials have been described in other publications.[8-12]

The electrical characteristics of ferrimagnetic materials that affect the design of magnetically tunable filters are these:

(1) Saturation magnetization, M_s*
(2) Anisotropy field constant, K_1/M_s
(3) Curie temperature, T_c
(4) Linewidth ΔH, or unloaded Q, Q_u
(5) Shape of sample.

Table III C-1

PROPERTIES OF SINGLE-CRYSTAL FERRIMAGNETIC MATERIALS FOR MAGNETICALLY TUNABLE FILTERS

MATERIAL	$4\pi M_s$ (AT ROOM TEMPERATURE) (gauss)	K_1/M_s (AT ROOM TEMPERATURE) (oersteds)	ΔH* (AT ROOM TEMPERATURE) (oersteds)	T_c (°C)
Yttrium-Iron-Garnet† (YIG)	1750	-43	0.22 (4 Gc, Ref. 14)	292
Gallium-Substituted† Yttrium-Iron-Garnet	50-1750 600 950 ± 50	-- -55.8 -41.7	-- -- 0.7-2.0 (at 4.4 Gc)	-- 160 206
Lithium Ferrite	3550 ± 40 (Ref. 9)	--	3§ (5 Gc)	--
"Planar" Ferrite "Zn_2Y" ($Ba_{12}Zn_2Fe_{12}O_{22}$)	2850 (Ref. 10)	4950 (Ref. 10)	10 (X-band, Ref. 10)	--

* These values of ΔH were measured in cavities. They may be considerably larger when measured in a filter structure. See discussion in Sec. C-2.

† These materials were supplied by Microwave Chemicals Laboratory, 282 Seventh Ave., New York City, New York.

§ Private communication, J. W. Nielsen, Airtron Division of Lytton Industries, Morris Plains, New Jersey.

Note that M_s, K_1/M_s, and T_c are intrinsic physical constants of the material.[13†] Table III C-1 lists the measured values of these physical constants. In the case of gallium-substituted yttrium-iron-garnet, M_s and K_1/M_s depend on the percentage of gallium substitution. The values of K_1/M_s given in the table were measured at SRI, at room temperature using two samples of Ga-YIG of different degrees of substitution of gallium. Values of the constants of the other materials in the table are taken from the indicated references.

---

* In m.k.s. units M_s is in ampere-turns per meter, and $\mu_0 M_s$ is in webers/meter^2, where $\mu_0 = 1.26\ (10^{-6})$ henries/meter. The unit $4\pi M_s$ in gauss is frequently used [$4\pi M_s$ (in gauss) $\times\ 10^{-4} = \mu_0 M_s$ (in webers/meter^2)].

† These constants vary with temperature. However, their value is independent of shape, frequency, and applied dc and RF fields.

The shape of the material affects the dc magnetic field required to produce resonance at a given frequency. In principle it is possible to achieve lower resonant frequencies by using an oblate spheroidal shape or a thin flat disc than by using a spherical resonator. The best resonators, *i.e.*, those having the highest Q_u have always in the past been achieved with spherical resonators. The effect of shape on the minimum resonant frequency is discussed below.

The significance of the Curie temperature T_c is that above this temperature the material suddenly loses its magnetic properties. Thus, operation above the Curie temperature will not be possible.

2. *Effect of Saturation Magnetization and Shape on Minimum Resonant Frequency*—The saturation magnetization M_s and the shape of the resonator determine the lowest resonant frequency, f_0^{min}, which can be reached. Figure III C-1 shows f_0^{min} of spheroidal resonators as a function of

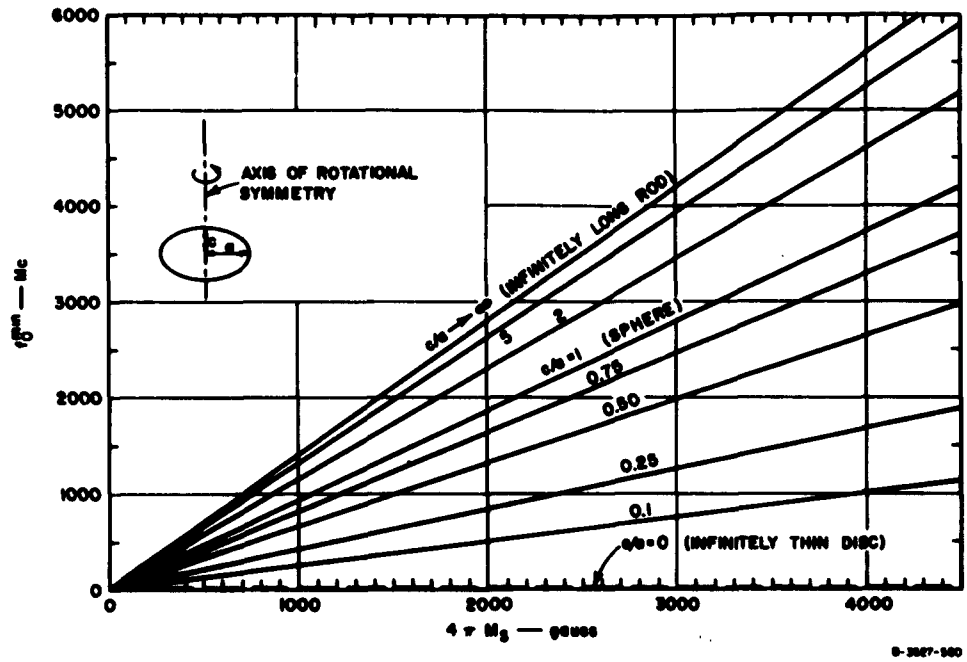

FIG. III C-1 MINIMUM RESONANT FREQUENCIES OF ELLIPSOIDS OF VARIOUS AXIS RATIOS

$4\pi M_s$ in gauss with the ratio of principal axes as a parameter. The most commonly employed resonator shape is spherical, which is primarily a result of the ease with which it can be fabricated and polished to give resonators with very high values of Q_u.

3. *Unloaded Q*, Q_u—The unloaded Q, Q_u, is usually given by the manufacturer in terms of an equivalent quantity, the linewidth ΔH.* To obtain Q_u from the linewidth, the following formula is used:

$$Q_u = \frac{f_0 \times 10^{-6}}{2.8\Delta H} \qquad \text{(III C-1)}$$

where

f_0 = Resonant frequency, cycles/second

ΔH = Linewidth, oersteds.

The Q_u of YIG increases about linearly with increasing frequency in the 2-10 Gc frequency range.[14] The values of Q_u obtained in a practical filter structure where the coupling is relatively tight, and consequently the conducting boundaries are near the resonator, are usually lower than the values specified for the material by the manufacturer. The value of Q_u varies substantially among the various configurations which have been tried. Figure III C-2 shows the values of Q_u that have been obtained with a 0.074-inch-diameter resonator in different coupling configurations, including a full-height S-band waveguide which is used as a reference to compare different resonators.

4. *Effect of Magnetocrystalline Anisotropy*—The effect of magnetocrystalline anisotropy is that the resonant frequency (or the biasing H-field required to yield a given resonant frequency) varies according to the orientation of the crystal axes with respect to the biasing magnetic field. Figure III C-3 shows the field required to resonate a YIG sphere at room temperature, as the resonator is rotated around a [110] crystal axis. The dc magnetic field is perpendicular to the axis of rotation of the sphere. For crystals with cubic symmetry (such as single-crystal YIG or gallium-substituted YIG)

* Linewidth is here defined as the difference between the two values of biasing field for which the imaginary part of the intrinsic susceptibility equals the real part, while frequency is held constant.

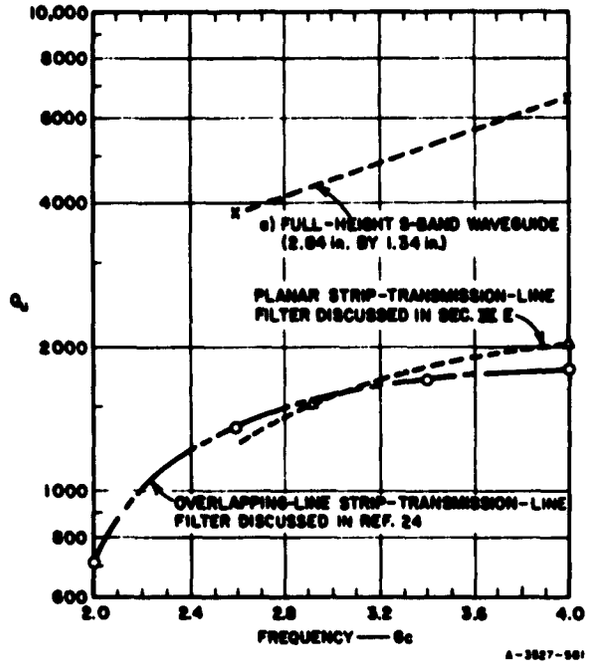

FIG. III C-2 Q_u OF YIG RESONATOR IN WAVEGUIDE AND STRIP-TRANSMISSION-LINE FILTER CONFIGURATIONS

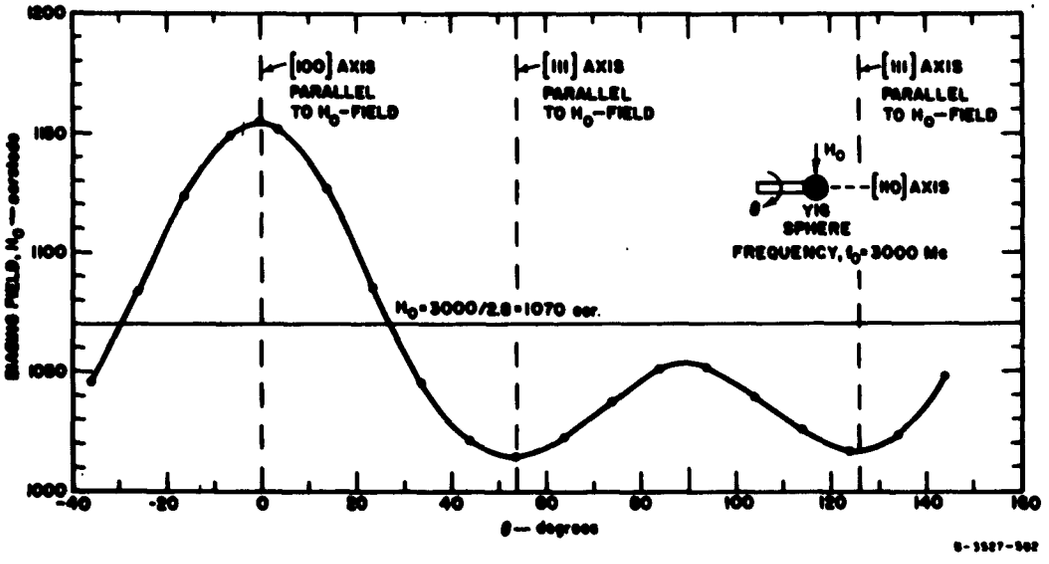

FIG. III C-3 FIELD STRENGTH TO GIVE RESONANCE AT 3000 Mc AS A YIG SPHERE IS ROTATED ABOUT AN [110] AXIS WHICH IS PERPENDICULAR TO H_0

$$H_0 = H_{eff} - \left(2 - \frac{5}{2}\sin^2\theta - \frac{15}{8}\sin^2\theta\right)\frac{K_1}{M_s} \quad \text{oersted} \qquad \text{(III C-2)}$$

where $H_{eff} = (f_0)_{mc}/2.8$, $(f_0)_{mc}$ is the resonant frequency in megacycles, and θ is the angle between H_0 and the [100] axis as the crystal is rotated about a [110] axis.

This resonant frequency variation which is due to magnetocrystalline anisotropy depends on the type of crystal structure and on the orientation of the crystal axes with respect to the dc magnetic field. Formulas for the resonant frequency have been given for several other different crystal structure types by Yager, *et al.*,[15] Kittel,[16] and Artman.[17]

The variation of the resonant field with crystal orientation has been suggested as a way to obtain synchronous tuning of three or more resonators where the center resonators are exposed to different boundary effects than those to which the terminal resonators are exposed.[18]

D. MAGNETICALLY TUNABLE FILTERS USING WAVEGUIDE COUPLING CIRCUITS

1. *Typical Structure*—The most promising structure, from the standpoint of achieving a minimum biasing magnet air gap and high off-channel isolation, appears to be overlapping waveguides. Figure III D-1 shows an example of this type of structure, which employs two resonators in waveguides having parallel axes. A slot in the common wall between

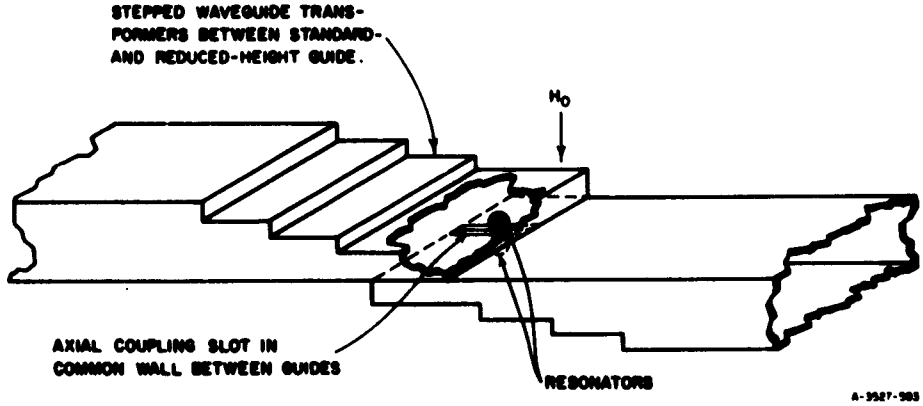

FIG. III D-1 TWO-RESONATOR FILTER USING OVERLAPPING WAVEGUIDE CONSTRUCTION

the two guides is used to provide coupling between the resonators; the slot is oriented parallel to the axis of the guides in order to give maximum isolation off resonance. In order to increase the coupling between the waveguides and the spheres, reduced-height waveguide is used in the region of the spheres, and step-transformers are used to provide a good impedance match into the reduced-height guides.

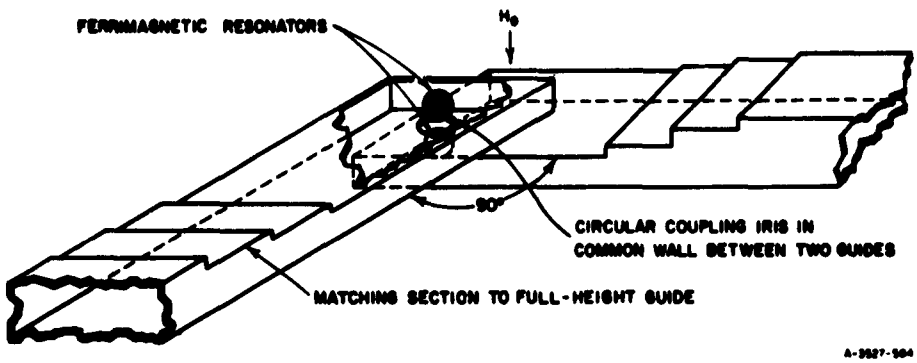

FIG. III D-2 TWO-RESONATOR FILTER USING OVERLAPPING GUIDES AT RIGHT ANGLES TO ACHIEVE HIGH REJECTION

Another possible structure is the crossed waveguide arrangement shown in Fig. III D-2.* A circular hole in the dividing wall near the short-circuited ends of the guides provides coupling between both RF magnetic moments of the resonators. At the same time the crossed waveguide arrangement eliminates the magnetic component of the coupling between the waveguides. Some small residual coupling between the waveguides due to electric fields may be expected.

Additional resonators may be incorporated in both of the above structures. This can be accomplished by placing these additional resonators in the coupling region between the resonators shown in Figs. III D-1 and III D-2, at the same time making the coupling iris thicker to provide the required spacing between the resonators.

* This structure was suggested by one of the authors (P. Carter), and K. R. Spangenberg and N. W. Federic of Physical Electronics Laboratories, East Palo Alto, California.

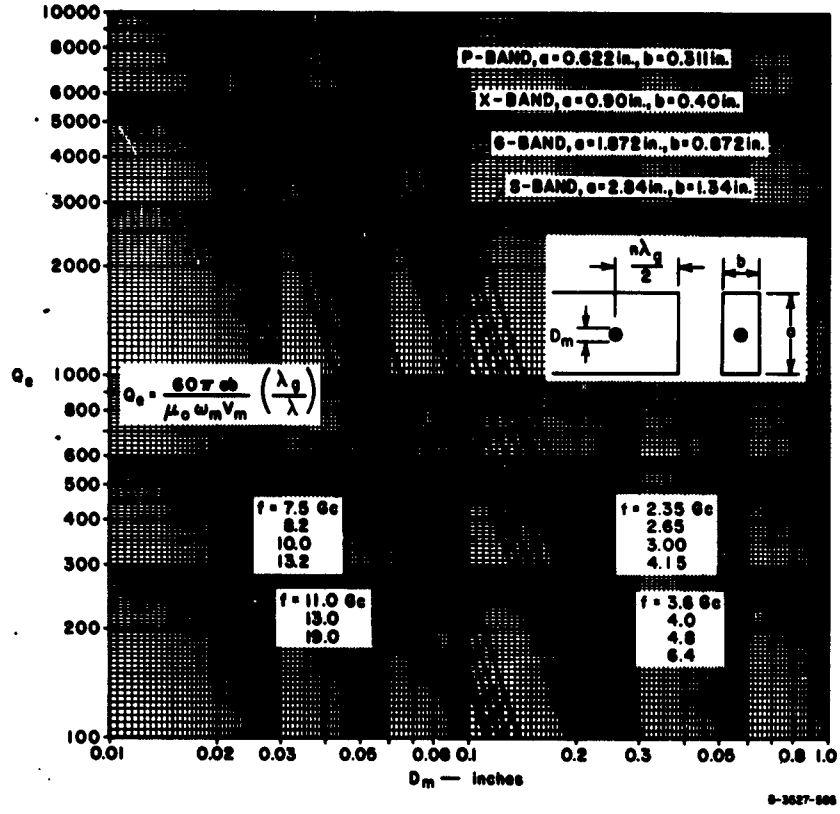

FIG. III D-3 Q_e vs. SPHERE DIAMETER OF SPHERICAL YIG RESONATOR LOCATED AT EQUIVALENT SHORT-CIRCUIT POSITION IN SHORT-CIRCUITED TE_{10} RECTANGULAR WAVEGUIDE

2. *Q_e Curves for Filters Employing Waveguide Coupling Structures*— The design of the waveguide coupling circuit for the input and output resonators is carried out using the curves shown in Fig. III D-3 which give the values of Q_e as a function of spherical resonator diameter for various standard rectangular waveguides. These curves were calculated from formulas given in a previous report,[4] for the case where the sphere is located at the center of the waveguide and close to the short-circuited end.*

These curves can be used to obtain Q_e when TE_{10}-mode rectangular guides of other than standard height are used, by applying the following simple transformation:

* The resonator may also be an integral number of half-wavelengths away from the short-circuit. For broad tuning ranges, however, the position close to the short-circuit is probably desirable.

$$Q_e' = Q_e \times \frac{b'}{b} \qquad \text{(III D-1)}$$

where

Q_e' = External Q in working guide

Q_e = External Q of standard guide, from Fig. III D-3

b' = Height of working guide

b = Height of standard guide.

The curves can also be used for all different shapes of ellipsoidal resonators. An equivalent sphere diameter D_n^e is used to replace D_n where

$$D_n^e = 2(abc)^{1/3} \qquad \text{(III D-2)}$$

in which a, b, and c are the semi-axes of the ellipsoid.

The curves are used for materials other than YIG, *e.g.*, Ga-YIG, by means of the following formula

$$Q_e^{OM} = \frac{M_s^{YIG}}{M_s^{OM}} \times Q_e^{YIG} \qquad \text{(III D-3)}$$

where

Q_e^{YIG} = External Q with YIG, from Fig. III D-3

Q_e^{OM} = External Q of material other than YIG

M_s^{YIG} = Saturation magnetization of YIG (1750 gauss at room temperature)

M_s^{OM} = Saturation magnetization of other material.

When the input and output waveguides have been designed to give the desired response and insertion loss, the filter is assembled. The dimensions of the coupling slot are adjusted experimentally to give the desired degree of coupling between the resonators.

The dimensions of the coupling slot that are required for a given value of coupling coefficient k depend on the spacing between the resonators and the size of the resonators. Generally it is desirable to

space the resonators as far apart as possible in order to minimize spurious responses. This procedure, however, leads to a large coupling slot and consequently to a lower off-channel rejection. A trade-off (determined largely by experimental procedures[18]) is therefore necessary between high off-channel rejection and spurious response.

The side-effects of the presence of the coupling iris in the common waveguide wall between the two resonators are: (1) to cause the values of Q_e to be higher than those which are shown in Fig. III D-3, and (2) to cause Q_u to be higher than that which is measured when the coupling iris is not present. The practical consequence of the existence of these two side-effects of the coupling slots is to require some additional experimental adjustment of the waveguide and/or resonator dimensions. Experience has shown that around 25-percent increase in the value of Q_e is obtained with typical coupling-slot configurations.

3. *Design Example of a Waveguide Filter*—A design is presented below which demonstrates the application of the above principles to the specification of the parameters for a filter with YIG resonators to operate in the frequency range 8.8-12.3 Gc. The requirements of this tunable filter are specified to be as follows:

$f_2 - f_1 = 42$ Mc

$Q_u = 2000$

Response shape—Tchebyscheff, 0.2-db ripple

Attenuation at 190 Mc from center frequency = 30 db

Tuning range—8.8 to 12.3 Gc.

The pass-band center frequency, f_0, varies as the filter is tuned magnetically, so that it is necessary to choose for design purposes a mean value of f_0 somewhere in the middle of the tuning range. A reasonable choice is the geometric mean of the limits of the tuning range $f_0 = \sqrt{8.8(12.3)} = 10.4$. We determine, using standard data for responses of lossless filters, that two resonators are needed to meet the bandwidth specification. The estimated mid-band dissipation loss is determined from Eq. (III B-4), inserting the low-pass prototype

parameters (g_i) for a two-pole low-pass filter with 0.2-db ripple ($g_0 = 1$, $g_1 = 1.0378$, $g_2 = 0.6745$, $g_3 = 1.5386$). Assuming $Q_u = 2000$, and inserting

$$w = \frac{f_2 - f_1}{f_0} = \frac{42}{10,400} = 0.00405 \quad ,$$

into Eq. (III B-4), we get a value of dissipation loss $L_d = 0.9$ db. The external Q's, $(Q_e)_A$, and $(Q_e)_B$ and the coupling coefficient k_{12} calculated from Eqs. (III B-1) and (III B-2) are,

$$(Q_e)_A = (Q_e)_B = 256$$

$$k_{12} = 0.0049 \quad .$$

Figure III D-3 is used to obtain the dimensions of the waveguide and the YIG resonators. Using full-height X-band waveguide, we see from the X-band 10-Gc line on the graph that in order to obtain a Q_e value of 256, as desired, spheres of about 0.090-inch diameter would be required if standard-height guide is used. Experience has shown that such large spheres will be very vulnerable to higher-order magnetostatic modes if operated at X-band. These modes result in spurious responses, which can be quite objectionable. For this reason let us consider the use of X-band guide with one-quarter of the standard height (*i.e.*, with $b' = 0.25 \times 0.400 = 0.100$ inch). Then by Eq. (III D-1) we wish to find the sphere diameter on the chart corresponding to $Q_e = Q_e' b/b' = 256 \cdot (0.400/0.100) = 1024$. From the X-band 10-Gc line in Fig. III D-3 we find that this height of guide requires 0.056-inch diameter YIG spheres. In order to allow for the effect of the adjacent slot on Q_e this sphere should be increased a little in size, say to about 0.060 inch. A sphere of this size should be considerably less vulnerable to higher-order magnetostatic mode activity, and this is a reasonable size to use. In order to match between the standard height and quarter-height guides a step transformer should be used as shown in Fig. III D-1.

If the YIG spheres are very close together, the presence of one sphere will distort the biasing H-field of the other, and vice versa. For this reason in this design it is desirable that the metal wall

between the two spheres be fairly thick (say, of a thickness roughly equal to or greater than the diameter of the spheres), in order to give adequate separation between the spheres. A wall thickness of 0.060 inch would be a reasonable choice in this case. The coupling slot between the spheres in Fig. III D-1 should have a length of several times the diameter of the spheres (say, 0.240 inch in this case) and a trial width of less than the diameter of the spheres (say, 0.040 inch in this case). After the filter is assembled, the coupling slot between spheres, by cut and try procedures, has its width increased until the desired coupling is obtained. The initial case with a 0.040-inch wide coupling slot will almost surely give an under-coupled response, *i.e.*, the response will have one point of minimum attenuation and will have appreciable reflection loss at that frequency. As the slot is made wider the reflection loss at the minimum attenuation point will become less until a perfect match is obtained at midband (except for a small VSWR due to circuit loss). If the slot is widened further, an over-coupled response will result, *i.e.*, there will be two points of minimum attenuation. Since a 0.2-db Tchebyscheff ripple was specified, the slot should be widened until such a ripple is obtained. This cut-and-try procedure is most easily carried out using a reflectometer and a swept generator.

If a waveguide device of bandwidth greater than a normal waveguide bandwidth is desired, a possible approach would be to use dielectric-slab-loaded guide[20] in the input and output sections. This may be preferable to ridge guide since ridge guide would require a larger magnet air gap.

E. STRIP-TRANSMISSION-LINE-COUPLED FILTERS

1. *A Single-Resonator Filter Configuration*—Figure III E-1(a) shows a configuration which has been applied quite widely to the design of single-resonator magnetically tunable filters and limiters.[21-23] The distance from the intersection of the strip-transmission-line center conductors to the short-circuit should be made as short as possible to minimize the electric coupling between the two transmission lines. Note that the two strip lines are at right angles to each other in order to maximize the off-resonance attenuation.

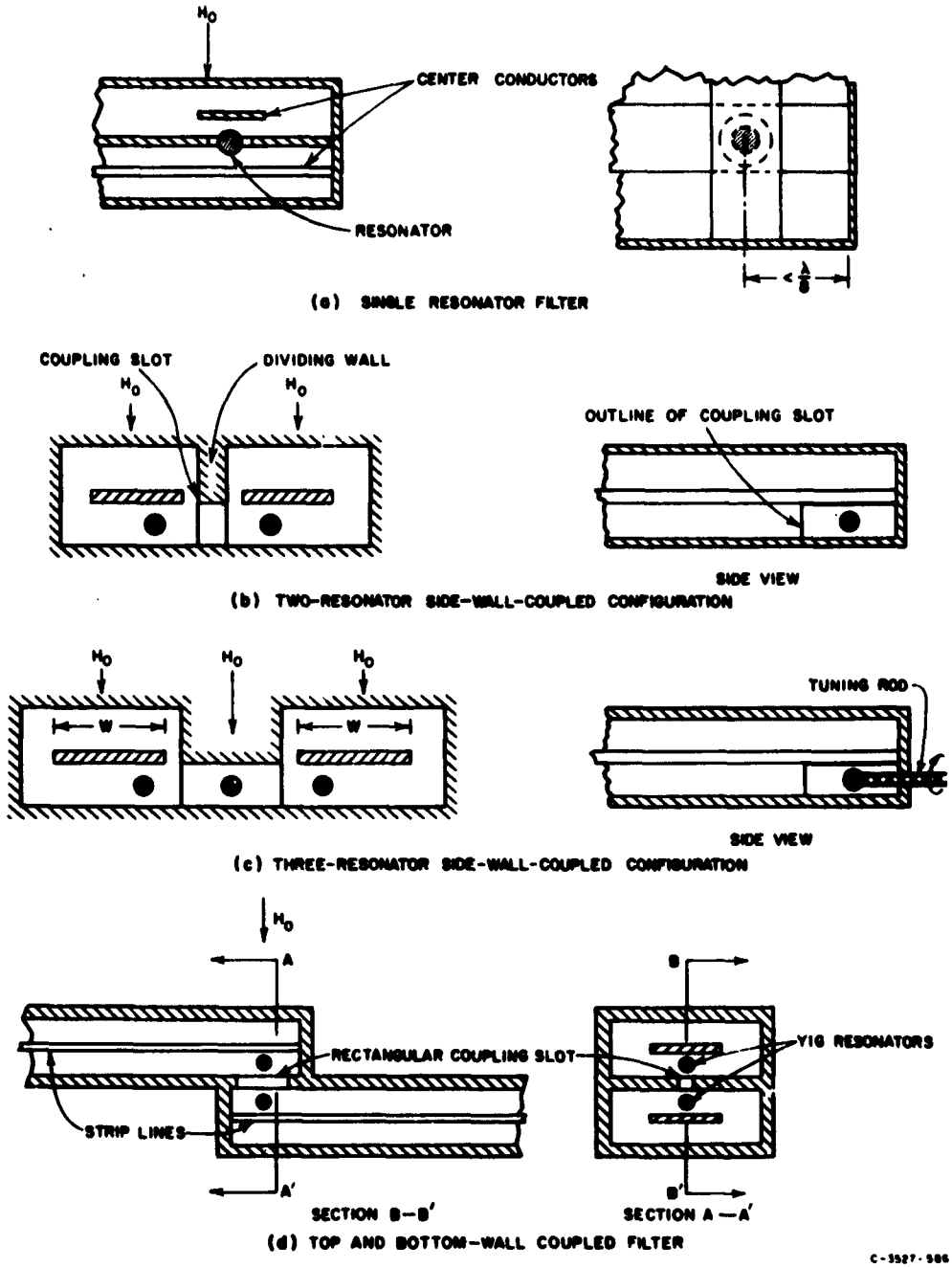

FIG. III E-1 SOME USEFUL CONFIGURATIONS FOR YIG FILTERS HAVING STRIP-LINE INPUTS AND OUTPUTS

2. *Multiple-Resonator Filter Configurations*—Figures III E-1(b), (c) and (d) show multiple-resonator filter configurations which have been operated in the *S*-band (2-4 Gc) range. The side-wall-coupled versions in Fig. III E-1(b) and Fig. III E-1(c) have the advantage that they require a minimum air gap distance over which the dc magnetic biasing field is applied. The top-and-bottom-wall-coupled filter shown in Fig. III E-1(d) has an advantage that good coupling can be obtained between resonators without moving them to the edges of the strip lines (which might help to excite higher-order magnetostatic modes). A version of this top-and-bottom-wall-coupled filter exhibited good insertion-loss, bandwidth, and off-channel rejection performance.[24] This configuration does, however, require a larger magnet air gap and probably might consume more electromagnet power than the side-wall-coupled version.*

3. *Design of YIG Filters with Strip-Line Inputs and Outputs*—The initial steps in the design of strip-transmission-line-coupled filters are the same as those used with waveguide-coupled filters. The resonator material is chosen on the basis of the minimum tuning frequency using Fig. III C-1, as explained in Sec. III-C. The values of $(Q_e)_A$ and $(Q_e)_B$ are obtained from Eq. (III B-1). Some allowance is made, as in the waveguide case, for the effect of the coupling slot, which usually causes Q_e to be higher than the theoretical value.

The strip-transmission-line dimensions are then determined which give the required values of $(Q_e)_A$ and $(Q_e)_B$. The first step is to obtain the spacing d between the strip center conductor and the ground plane, and the resonator diameter D_s. Figure III E-2 gives theoretical data from which the required spacing d can be determined for a given spherical resonator diameter, where the strip line is of 50 ohms impedance. In general it is desirable to keep the ratio of the resonator diameter to the spacing d as small as possible in order to minimize the deleterious effect of the conducting surfaces on Q_u. However, in order to obtain adequately low Q_e values one cannot make the ratio D_s/d too small.

---

* This tentative conclusion, that the side-wall-coupled version would require less bias magnet power than the top-and-bottom-wall-coupled versions is based on the following reasoning. Although the volume occupied by the resonators is approximately the same for both filter configurations, there will be more energy required to bias the top-and-bottom-wall-coupled version, because of the substantial amount of field energy stored in fringing fields, outside the region between the pole faces.

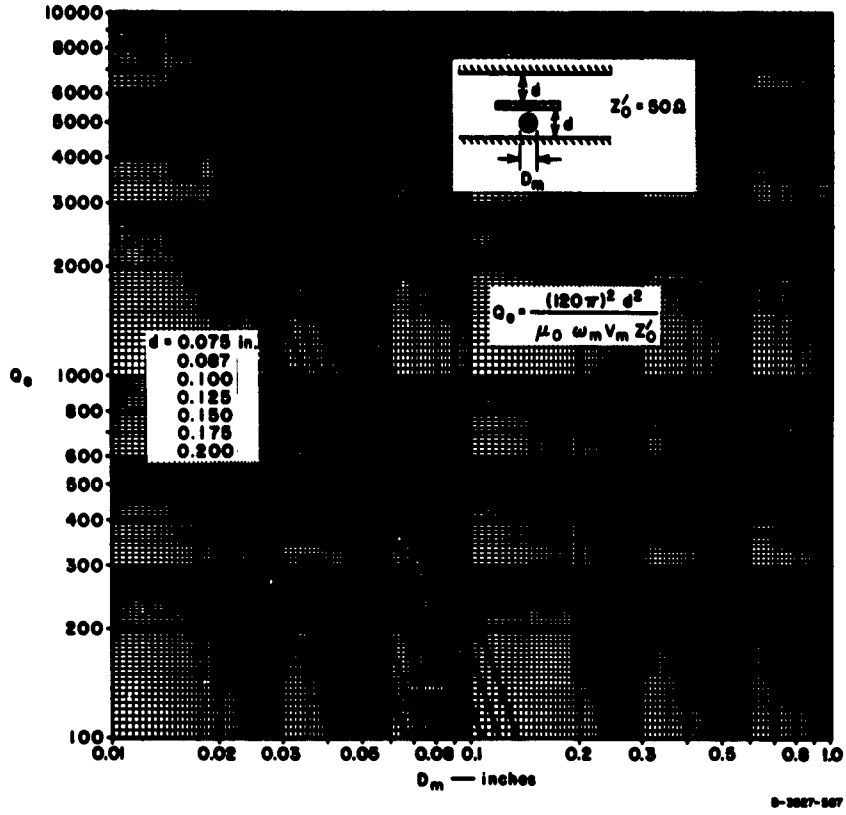

FIG. III E-2 Q_e vs. SPHERE DIAMETER FOR SPHERICAL YIG RESONATOR IN SYMMETRICAL STRIP-TRANSMISSION-LINE

For the configuration Fig. III E-1(b), the remaining strip-transmission-line dimensions $S_1/2$, $S_2/2$, and W, shown in Fig. III E-3, are determined from charts of fringing capacitance given by Getsinger.[25] The thickness, t, of the line is chosen as small as possible to minimize these fringing capacitances. Also, $S_2/2$ is chosen to be large enough so that further increasing this dimension does not appreciably decrease the fringing capacitance C_{f0}^2 which it contributes. Similarly, a value of $S_1/2$ which does not add an excessive amount of fringing capacitance C_{f0}^1 compared to the total line capacitance C_t is chosen. The width W is calculated from the following formula:

$$\frac{W}{b} = \frac{1}{2}\left(1 - \frac{t}{b}\right)\left(\frac{C_t}{\epsilon} - \frac{C_{f0}^1}{\epsilon} - \frac{C_{f0}^2}{\epsilon}\right) \qquad \text{(III E-1)}$$

in which ϵ is the dielectric permittivity of region between center conductor and shield, and b is the ground plane spacing.

4. *Design Example of a Two-Resonator Strip-Transmission-Line-Coupled Filter*—Suppose that the following characteristics are required of a two-resonator filter:

Tuning range—2 Gc to 4 Gc

Bandwidth between 3-db attenuation frequencies—20 Mc

Type of response—Maximally flat

Type of structure—Side-wall-coupled resonators.

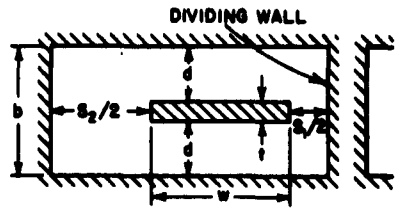

FIG. III E-3 LINE DIMENSIONS USED IN INPUT AND OUTPUT SECTIONS OF SIDE-WALL-COUPLED RESONATOR FILTER

From Eq. (III B-1)

$$(Q_e)_A = (Q_e)_B = \frac{\omega_1' g_1 g_0}{w} = \frac{1 \times 1.414 \times 1}{0.0071} = 202$$

where

$$w = \frac{f_2 - f_1}{f_0} = \frac{20}{2820} = 0.0071$$

$f_0 = 2820$ Mc is the geometric mean of the limits of the tuning range $= \sqrt{2000 \times 4000}$. From Eq. (III B-3),

$$k_{12} = \frac{w}{\omega_1' \sqrt{g_1 g_2}} = \frac{0.0071}{1 \times \sqrt{(1.414)^2}} = 0.00495 .$$

k_{12} is realized experimentally by adjustment of the dimensions of the coupling iris.

The resonator material is chosen using the requirement that the minimum center frequency is 2 Gc. From Fig. III C-1 a maximum $4\pi M_s$ of 2150 gauss for a spherical resonator is seen to be allowable. Yttrium-iron-garnet ($4\pi M_s = 1750$ gauss) satisfies this requirement; furthermore its unloaded Q, Q_u is quite high at frequencies as low as 2 Gc (see Fig. III C-2). We then obtain the strip-transmission line center-conductor-to-ground-plane spacing from Fig. III E-2 using $Q_e' = 150$ in order to allow for a 33 percent increase due to the effect of

the coupling iris. We choose the following combination of resonator diameter and ground-plane spacing:

$$D_a = 0.074 \quad \text{inch}$$

$$d = 0.110 \quad \text{inch} \quad .$$

We follow the procedure outlined in Sec. III E-2 for calculating the strip-transmission-line dimensions. We choose

$$t = 0.011 \quad \text{inch (\#29 gauge)}$$

$$S_1/2 = 0.025 \quad \text{inch}$$

$$S_2/2 = 0.100 \quad \text{inch}$$

$$b = 2d + t = 0.2312 \quad \text{inch} \quad .$$

These choices give the following values of the fringing capacitances

$$\frac{C_{f0}^1}{\epsilon} = 1.1$$

$$\frac{C_{f0}^2}{\epsilon} = 0.56 \quad .$$

Inserting these values in Eq. (III E-1) we get

$$W = 0.231 \quad \text{inch} \quad .$$

The final cross-sectional dimensions of the strip-transmission-line coupling section are given in Fig. III E-3.

F. CONSTRUCTION AND TESTING OF AN EXPERIMENTAL STRIP-TRANSMISSION-LINE-COUPLED FILTER

1. *Construction*—The design example given in Part E was used to construct an experimental two-resonator filter. Figure III F-1 shows the important dimensions and arrangement of elements in the filter.

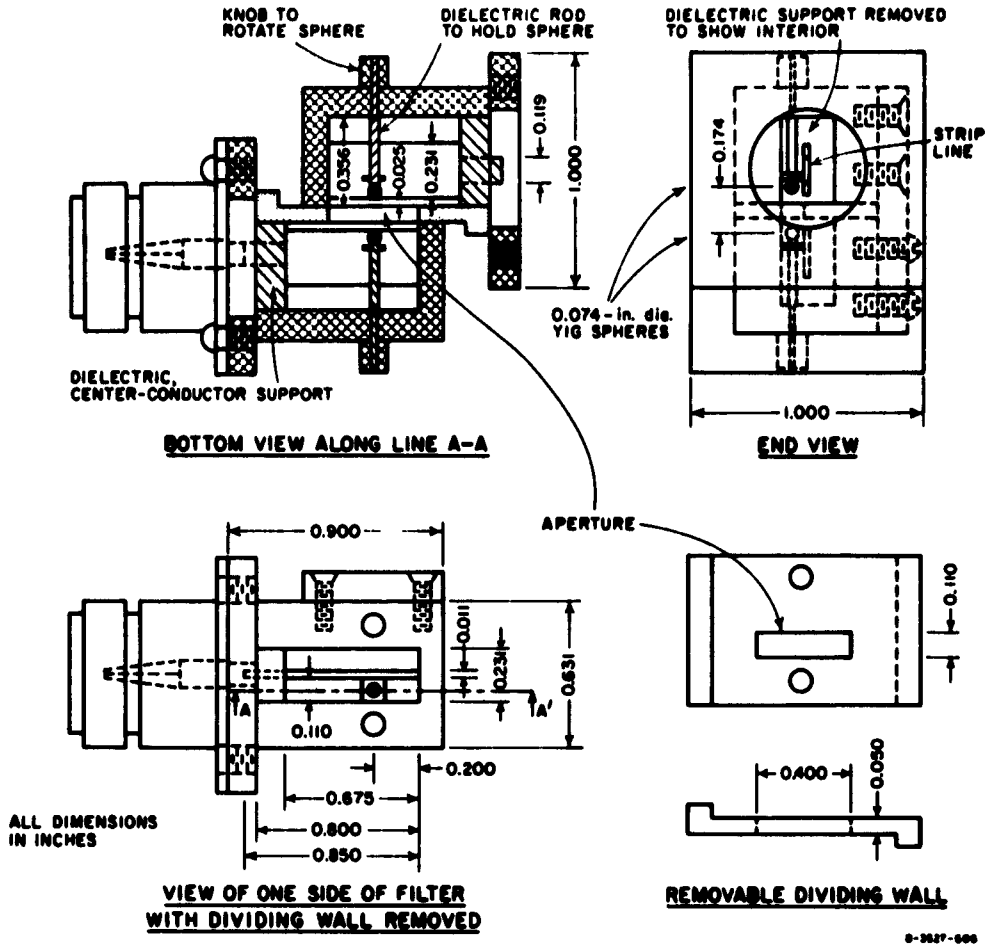

FIG. III F-1 SIDE-WALL-COUPLED FILTER

The two 0.074-inch diameter YIG resonators were attached to two tuning rods as shown in Fig. III F-1. The tuning rods were attached along a [110] axis of each YIG crystal, using the orientation technique described in a previous reference.[18]

The strip-transmission-line input and output sections were constructed so that the filter could easily be disassembled for modification, such as changing the dimensions of the coupling slot or replacing the resonators with different materials and resonator sizes. With this type of construction, *i.e.*, using a demountable coupling plate, the filter could easily be modified to construct the three-resonator filter which is described in Part G.

2. *Tuning of the Two-Resonator Filter*—In two-resonator filters such as the ones that have been described in previous reports, the resonators were synchronously tuned by lining them up with their easy axes of magnetization parallel to the dc magnetic field. In the case of the two-resonator filter the boundary conditions "seen" by two identical resonators are the same to within the tolerances of the dimensions of the strip-transmission lines and coupling iris. The difference in the resonant frequencies of the two resonators is kept to within 2 or 3 Mc by using ordinary machining tolerances. In the case of the three-resonator filter (to be discussed later), the center resonator sees different boundary conditions from those seen by the end resonator, and therefore it requires some tuning compensation. It is for this reason, *i.e.*, to provide a means for tuning the three-resonator version of this filter, that tuning rods were attached to the input and output resonators of this two-resonator filter.

The tuning procedure for the two-resonator filter is as follows: First, one of the resonators is removed from its mounting in the filter. The filter is assembled and operated as a single-resonator filter in which the output is very loosely coupled to the resonator, through the coupling iris. The resonator is rotated while at the same time the output of the filter is observed, keeping the frequency constant. At each position of the rotation of the resonator a value of dc magnetic field is found at which maximum output of the filter occurs. The results of this procedure can be represented by a tuning curve such as the one shown in Fig. III C-3. The absolute values of the dc magnetic field required to tune the filter will be somewhat lower than those shown in Fig. III C-3 since the data in Fig. III C-3 were taken in full-height waveguide and do not include the field-lowering effects of the nearby conducting walls of the filter.

The tuning rod is now adjusted to give a value of dc magnetic field which is about half way between the minimum and maximum values. The second resonator is now mounted in the filter and rotated until maximum output is obtained. The alignment procedure was carried out at 3.0 Gc. This tuning frequency was used in order that any departure from synchronous tuning of the two resonators will be minimized in the 2- to 4-Gc range. It should be noted that when the filter is mounted within a magnet that the direction of the biasing H field must be accurately the same as when the filter is tuned or the resonators may become detuned.

3. *Discussion of Experimental Results*—Figures III F-2 and III F-3 show the response curves of the filter when it was tuned successively to three different center frequencies, 2.000 Gc, 3.000 Gc, and 4.000 Gc. Table III F-1 gives some of the other filter parameters, which are discussed in more detail below.

Table III F-1

MEASURED AND CALCULATED CHARACTERISTICS
OF TWO-RESONATOR SIDE-WALL-COUPLED FILTER

f_c (Gc)	$(L_A)_{min}$ (db)	$VSWR_c$	Q_u (CALCULATED FROM MEASURED DATA)	k_{12} (CALCULATED)	H_0 (oersteds)	$\Delta f^*_{3\ db}$ (Mc)	$\Delta f^*_{30\ db}$ (Mc)	Q_e
2.000	4.0	1.9	--	--	714.7	26	117	--
3.000	1.2	1.01	1500	0.00472	1070	20	113	212
4.000	1.0	1.48	2050	0.00424	1427	25	121	236

* The bandwidths given are measured to the 3-db or 30-db points below $(L_A)_{min}$.

Single-peaked responses (see Fig. III F-2) were obtained at f_0 = 3.000 Gc and 4.000 Gc. The VSWRs at these two center frequencies are 1.01 and 1.48 respectively, indicating that the coupling was nearly critical and giving a maximally flat response. Note that a double-peaked response was obtained at 2 Gc.

The experimental response data around band center were used to calculate the Q_u of the resonators, assuming that the Q_u's are equal,* and that the frequency response shape is maximally flat. The values of Q_u calculated from the response are shown in Table III F-1 and also in Fig. III C-2.

The Q_u of the resonators in this structure compares favorably with the Q_u of the same pair of resonators when they were mounted in the overlapping line strip-transmission-line filter previously reported.[24] These values of Q_u for the overlapping construction were also shown in Fig. III C-2. That filter had a 0.095-inch spacing between the strip center-conductor and the ground plane. One might have expected a higher Q_u to be obtained

* It was shown in a previous report (see Table II-1 of Ref. 24) that the Q_u of these two resonators are approximately equal.

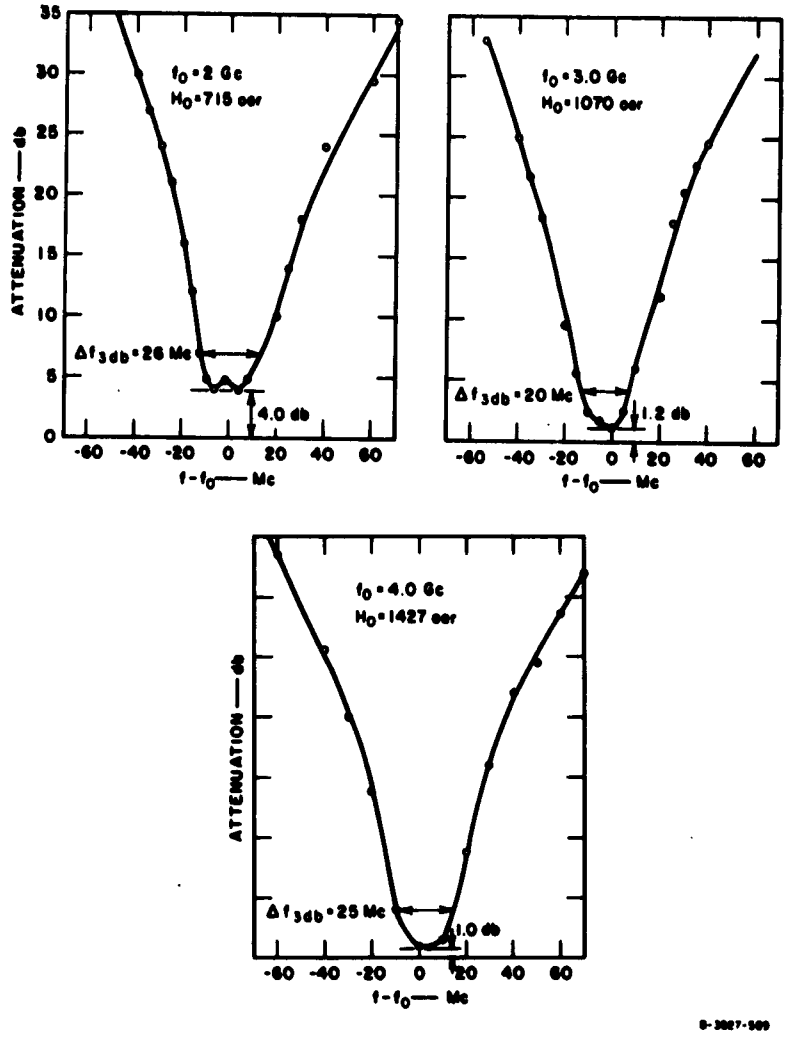

FIG. III F-2 PASS-BAND CHARACTERISTICS OF THE TWO-RESONATOR FILTER IN FIG. III F-1

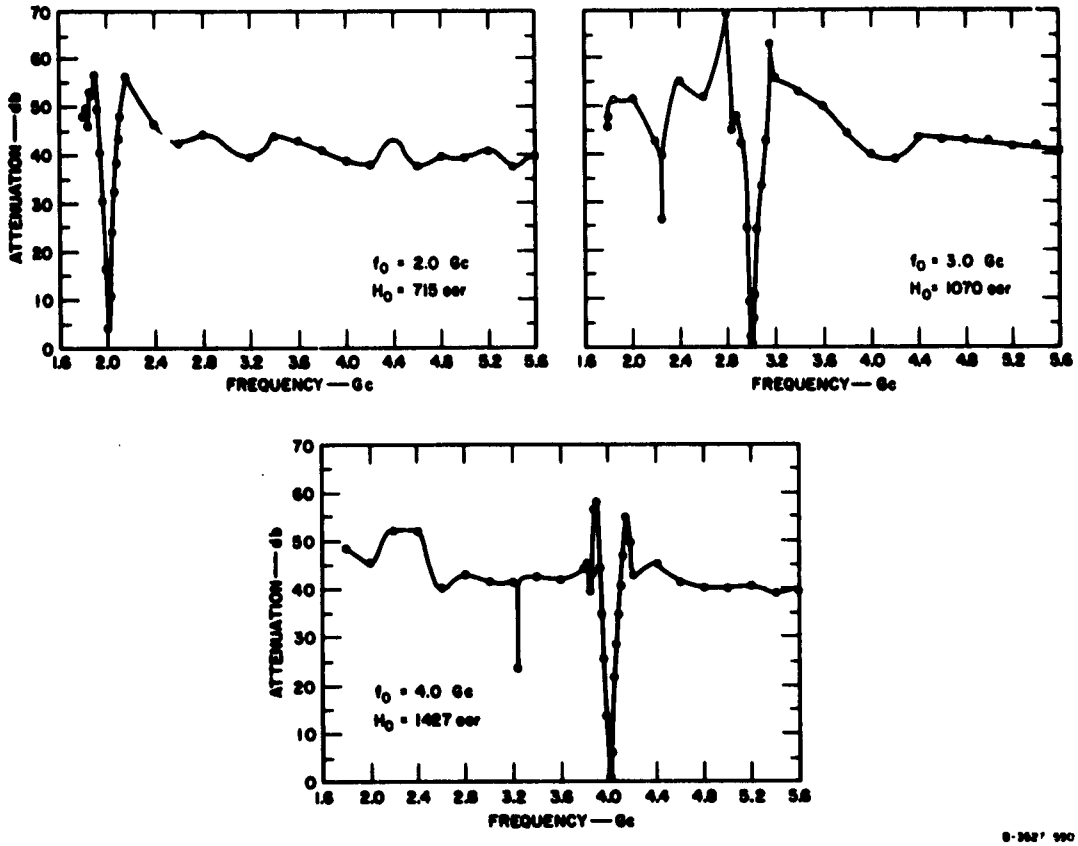

FIG. III F-3 STOP-BAND CHARACTERISTICS OF THE TWO-RESONATOR FILTER IN FIG. III F-1

with the present greater center-conductor-to-ground-plane spacing (0.110 inch). Such was not the case, however; the relative lower Q_u in the present side-wall-coupled version may be due to the close proximity of the dividing wall above the coupling slot and also to the fact that the coupling slot in the overlapping line version was cut in the ground-plane directly beneath the resonator. It was shown[24] on the overlapping-line filter that the effect of the coupling slot in this position was to increase the values of Q_u to about 30 percent greater than those obtained when the coupling slot was replaced with smooth conducting ground-plane.

This side-wall-coupled filter has a narrower pass band and a lower insertion loss than the previously reported side-wall-coupled filter.[19] Part or all of the improvement in midband attenuation may be due to

the fact that one of the resonators used in the previous filter had a lower Q_u than either of the two resonators used in this filter.

The off-channel rejection at 60 Mc below band center at 2.0 Gc, 3.0 Gc, and 4.0 Gc center frequencies is 41 db, 40 db, and 33.5 db, respectively. This amount of rejection would be quite useful for an image response suppression in a tunable microwave receiver which had a 30 Mc IF frequency.

A single spurious response occurs at a frequency which is 760 Mc below the band center. This spurious response has recently been identified with considerable certainty to be due to the resonance of the 210 magnetostatic mode. The procedure used for identifying this mode is useful since in this case, and possibly in others, it suggests a method by which the spurious response may possibly be eliminated. The identification is based on a comparison between the dc magnetic fields required to resonate the uniform precession, *i.e.*, the main response, and the higher-order mode spurious response. The theoretical values of these resonating fields have been calculated for many of the magnetostatic modes of a ferrimagnetic sphere and mode charts have been plotted which are useful for mode identification.[28]

The field required to resonate the uniform precessional resonance mode is strongly influenced by the presence of the conducting boundaries of the strip transmission line. The same influence affects the resonating fields required for the higher order magnetostatic modes. This effect makes the identification of the modes from the absolute values of the resonating fields rather difficult. We note, however, in Fig. III F-3 that the difference in frequency between the main resonance, *i.e.*, band center, and the most prominent spurious response is constant, and equal to 760 Mc. If we examine a magnetostatic mode chart of the type published by Fletcher[28] we observe that the 210 mode is approximately 650 Mc away from the uniform precessional resonance mode for a zero-anisotropy ferrite. The 110 Mc discrepancy might be explained by boundary effects, by anisotropy or by a combination of both. Further evidence that this 210 mode identification is correct is obtained (1) from a study of the dc magnetic fields required for resonance with fixed frequency, and (2) from a study of the distribution of RF magnetization in the suspected mode. For a study of the fields, data from Fig. IV E-2 of Ref. 8 is used. Table III F-2 gives values of the fields $H_0^{(110)}$ and $H_0^{(210)}$ at the peaks of the main

Table III F-2

IXC MAGNETIC BIASING FIELDS AT MAIN AND SPURIOUS RESPONSE PEAKS

Data taken from Fig. IV E-2 of Ref. 8

f_0 (Gc)	$H_0^{(110)}$ (oersteds)	$H_0^{(210)}$ (oersteds)	$H_0^{(210)} - H_0^{(110)}$ (oersteds)
2.100	470	730	260
3.100	780	1025	245
3.900	1080	1290	210

response and strongest subsidiary response, respectively, of the side-wall-coupled filter discussed in Ref. 8. The theoretical value of $H_0^{(210)} - H_0^{(110)}$ is 235 oersteds, and is independent of the frequency and of the anisotropy.[27] This value compares quite closely to the experimental values in Table III F-2.

Figure III F-4 is a cross section of a ferrimagnetic sphere showing the distribution of the m_x component of RF magnetization of the 210 mode. The RF magnetization is circularly polarized, *i.e.*, $m_y = jm_x$ and there is no variation of either m_x or m_y in the x or y directions. The RF magnetization is a linear function of the vertical distance z from the equatorial plane of the sphere. Excitation of this mode could therefore be eliminated and this spurious response avoided by locating the resonator in an RF driving field which has even symmetry with respect to the equatorial plane. One way to achieve this would be to use a balanced transmission line type of coupling structure, where the resonator was mounted between the center conductors, as shown in Fig. III F-5. This type of transmission-line structure has a symmetry plane through the center of the structure and through the equatorial plane of the resonator. The main disadvantage in this particular structure is that it requires the use of a very broad-band balancing network

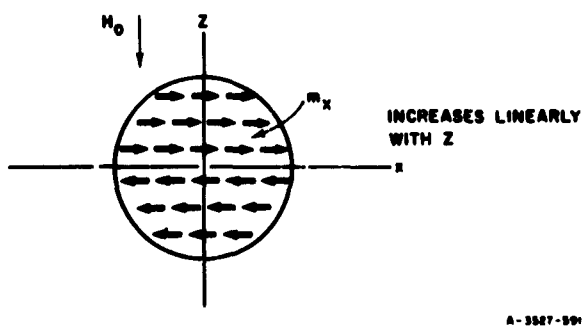

FIG. III F-4 DISTRIBUTION OF THE RF MAGNETIZATION IN THE 210 MODE

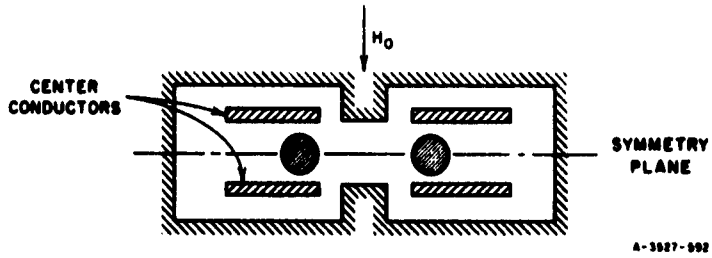

FIG. III F-5 A POSSIBLE STRUCTURE TO ELIMINATE THE 210 MODE SPURIOUS RESPONSE

to transform between the coaxial line input and the balanced strip-transmission line structure. One such balancing network has been reported.[29]

The bandwidths between 3-db insertion-loss frequencies and between 60-db insertion-loss frequencies, which are listed in Table III F-1, are nearly the same at all three center frequencies. The slightly larger 3-db bandwidth at f_c = 2.0 Gc may be due to the detuning of the resonators, as discussed above. It is not well understood why this constant bandwidth occurs, since it requires that the coupling coefficient k_{12} between the resonators decrease and that the external Q, Q_e increase by equal factors as the center frequency is increased, *i.e.*, that $k_{12}Q_e$ = constant. As the frequency is increased, the strip-transmission-line conducting boundaries must exert a greater shielding effect on the resonator, causing it to couple less strongly to the center conductor and also to couple less strongly to the other resonator by way of the coupling slot.

The values of the external Q_e which are obtained by calculation from the measured responses at 3.0 Gc and 4.0 Gc are equal to 212 and 236 respectively. These measured Q_e's compare reasonably well with the theoretical value Q_e = 200 given by Fig. III E-2. The validity of the procedure used to design the transmission line coupling section to give a designated value of Q_e appears to thus be further validated by the measured results which were obtained with this filter.

The attenuation of this filter at frequencies far away from the pass-band center frequency depends entirely on the dimensions, *i.e.*, thickness, length, and height of the slot in the side wall between the

resonators. It is desired, as a design objective, to achieve the maximum attenuation that is possible with a given degree of coupling between the resonators. If we examine this coupling problem we see that the following guidelines may be followed to achieve this objective of high off-channel attenuation:

(1) Make the slot as long as practical,

(2) Make the height of the slot as small as possible and the thickness as large as possible,

(3) Place the resonators as close to the slot as possible consistent with other requirements, namely, spurious mode suppression.

The reasoning behind the first two guidelines is as follows: Up to a point, lengthening the coupling slot will increase the coupling between the spheres with relatively little effect on the off-pass-band attenuation. The coupling slot should therefore be made as long as possible in order to achieve the desired inter-resonator coupling. The maximum length of the slot is limited to twice the distance between the center of the resonator and the short-circuit, because the input and output lines are brought in from opposite directions. If the two lines were placed side by side with their inputs at the same end of the filter, the coupling slot could be made even longer to obtain the maximum amount of inter-resonator coupling with a given minimum off-channel rejection.

The shielding, *i.e.*, coupling between the two lines can be interpreted in terms of the coupling between the electric or magnetic field lines of the two center conductors. It is apparent that, since the resonator is directly adjacent to the coupling slot and the strip transmission line is above the resonator, reducing the height of the slot will reduce the coupling between the center conductors more than it reduces the coupling between the resonators.

Close spacing between the resonators is desirable according to Guideline (3) above so that the slot can be made thick and narrow according to Guidelines (1) and (2). The inter-resonator spacing may not, however, be reduced below that spacing which starts to cause excessive spurious responses or which starts to degrade the Q_u excessively.

These guidelines in the design of the coupling slot were recognized and followed in the design of this version of the side-wall-coupled

filter. Some previous experimental study of the effect of varying the dimensions of the coupling slot in the side-wall-coupled filter has already been reported which confirms these guidelines.[18]

G. DESIGN, CONSTRUCTION, AND TESTING OF THREE-RESONATOR FILTER

Additional resonators are often required in band-pass filters in order to increase the rate at which the attenuation increases with frequency outside of the pass band. The addition of a third resonator enhances this "skirt selectivity," as it is sometimes called, considerably. For instance, with a 1-db ripple overcoupled response, the ratio of the 30-db bandwidth of the two-resonator case to the 30-db bandwidth of the three-resonator case is 4.7:2.3 = 2.43. This increase in selectivity is often gained at a negligible cost in increased pass-band center-frequency attenuation.

1. *Design and Construction of Center Resonator Section*—The addition of a third resonator to the two-resonator side-wall-coupled filter configuration was accomplished quite simply in this case by replacing the two-resonator filter coupling plate with a center section containing the center resonator. The end result was to convert a two-resonator structure of the form in Fig. III E-1(b) into a three-resonator structure of the form in Fig. III E-1(c). The height of the region containing the middle resonator was made the same as the spacing between the strip lines and the ground planes. In this manner the center resonator sees boundary conditions very similar to those seen by the end resonators. The thickness of the plate containing the center resonator was chosen so that the three spheres would be spaced by an amount approximately equal to the spacing between the spheres in the two-resonator design. In this particular filter this gave satisfactory results though in some cases further adjustment of the sphere spacing might be desirable in order to obtain a desired response shape. As shown in Fig. III G-1, the length of the region containing the center resonator was made to be 0.400 inch, the same as the length of the coupling slot in the previous two-resonator version of this filter. The center resonator was mounted on a 0.062-inch diameter Rexolite rod, which was in turn inserted through and glued to a brass mounting plug. The resonator was mounted so that its [110] crystal axis was parallel to the Rexolite rod,[18] so that the resonator could be tuned in the same manner that the end resonators were

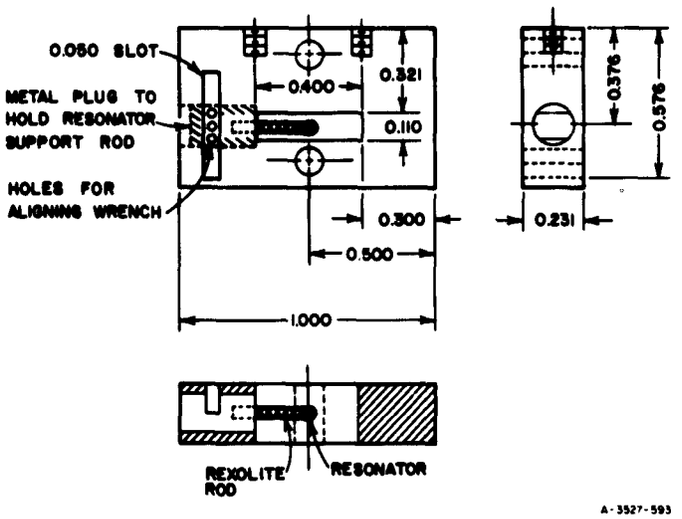

FIG. III G-1 CENTER SECTION OF THREE-RESONATOR FILTER

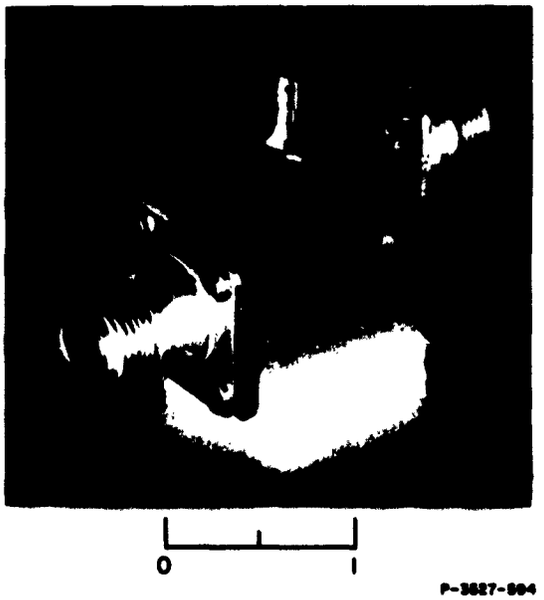

FIG. III G-2 PHOTOGRAPH OF THE ASSEMBLED THREE-YIG-RESONATOR FILTER SHOWN WITHOUT A MAGNET

tuned. The block with the center resonator shown in Fig. III G-1 was used to replace the dividing wall and coupling slot in Fig. III F-1. The assembled three-resonator filter is shown in Fig. III G-2. The rod protruding at the top was used for rotating the adjacent end resonator in order to tune it, as previously discussed.

2. *Tuning of Three-Resonator Filter*—The following procedure was used to align the three resonators to obtain synchronous tuning. The center resonator was removed and the two input and output resonators were rotated on their tuning rods to obtain synchronous tuning at a position such that the dc magnetic field required was approximately midway between the minimum and maximum values on the tuning curve. The condition of synchronous tuning was determined by measuring the insertion loss of the structure, minus the center resonator, as a function of field. The circuit gives a sharp single-peaked response when the two resonators are synchronously tuned; otherwise it yields a double-peaked response. The third center resonator was then added and was tuned until a three-peaked response resulted. This tuning procedure was carried out at $f_0 = 3.0$ Gc. The tuning rods were thereafter affixed securely to the body of the filter with the epoxy cement.

The input and output resonators in the three-resonator filter were in the same position that they occupied in the two-resonator filter. The center resonator was placed in the middle of the filter section. The distance between the centers of adjacent resonators was therefore 0.177 inch. This distance is almost exactly the same as the distance between the centers of the resonators of the two-resonator filter.

3. *Performance of Three-Resonator Filter*—The responses of the filter were measured at several center frequencies throughout the 2.0-8.0 Gc frequency range. These performance data are shown in Figs. III G-3 and III G-4. The response data were taken in all cases by varying the dc biasing field while keeping the frequency constant. By this means the problems of detector calibration and variation of signal generator output over a wide band of frequencies were avoided. The responses around band center shown in Fig. III G-3 were measured by automatically sweeping the biasing field across the resonant field value for the given signal frequency. The output of the crystal was fed into a logarithmic, strip recorder which had a 40-db dynamic range. Besides measurements

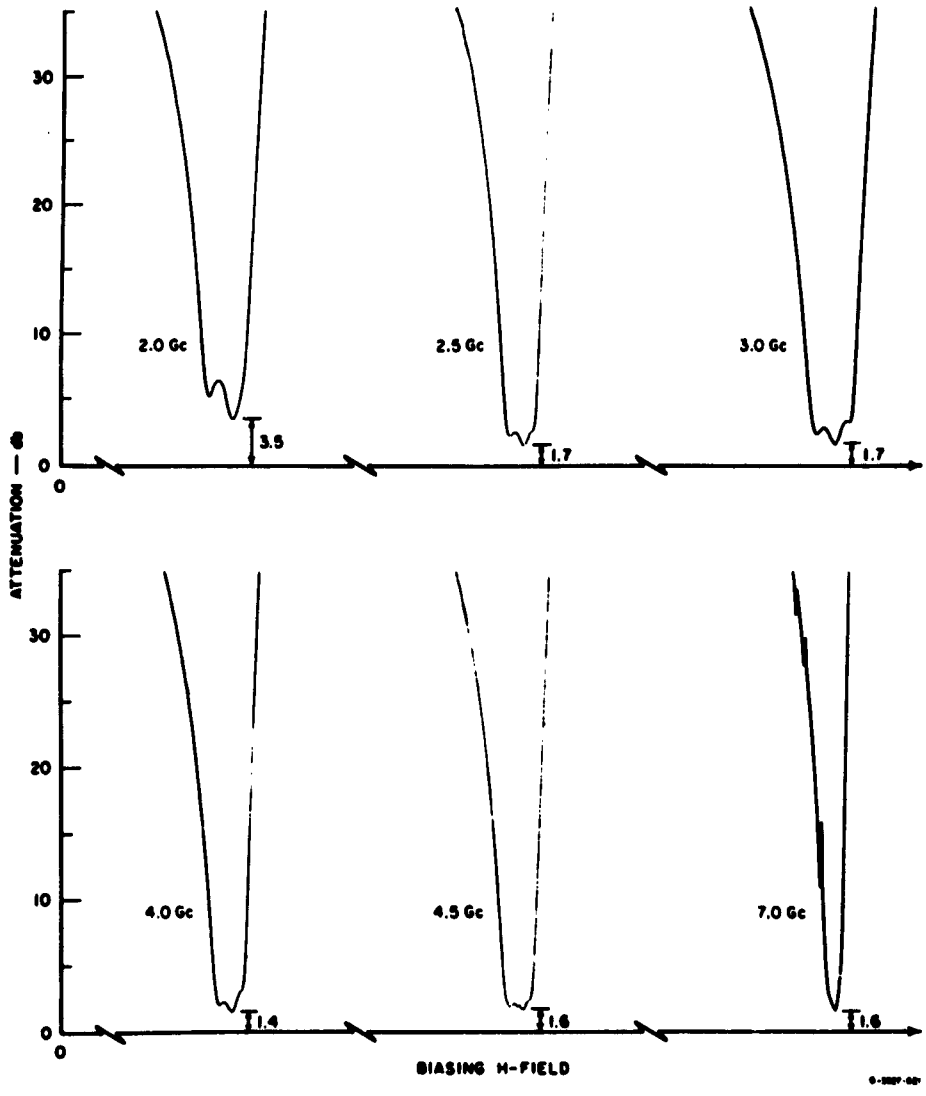

FIG. III G-3 ATTENUATION vs. BIASING H-FIELD FOR THREE-YIG-RESONATOR FILTER IN FIG. III G-2
These curves were obtained using a recorder and a swept magnet power supply

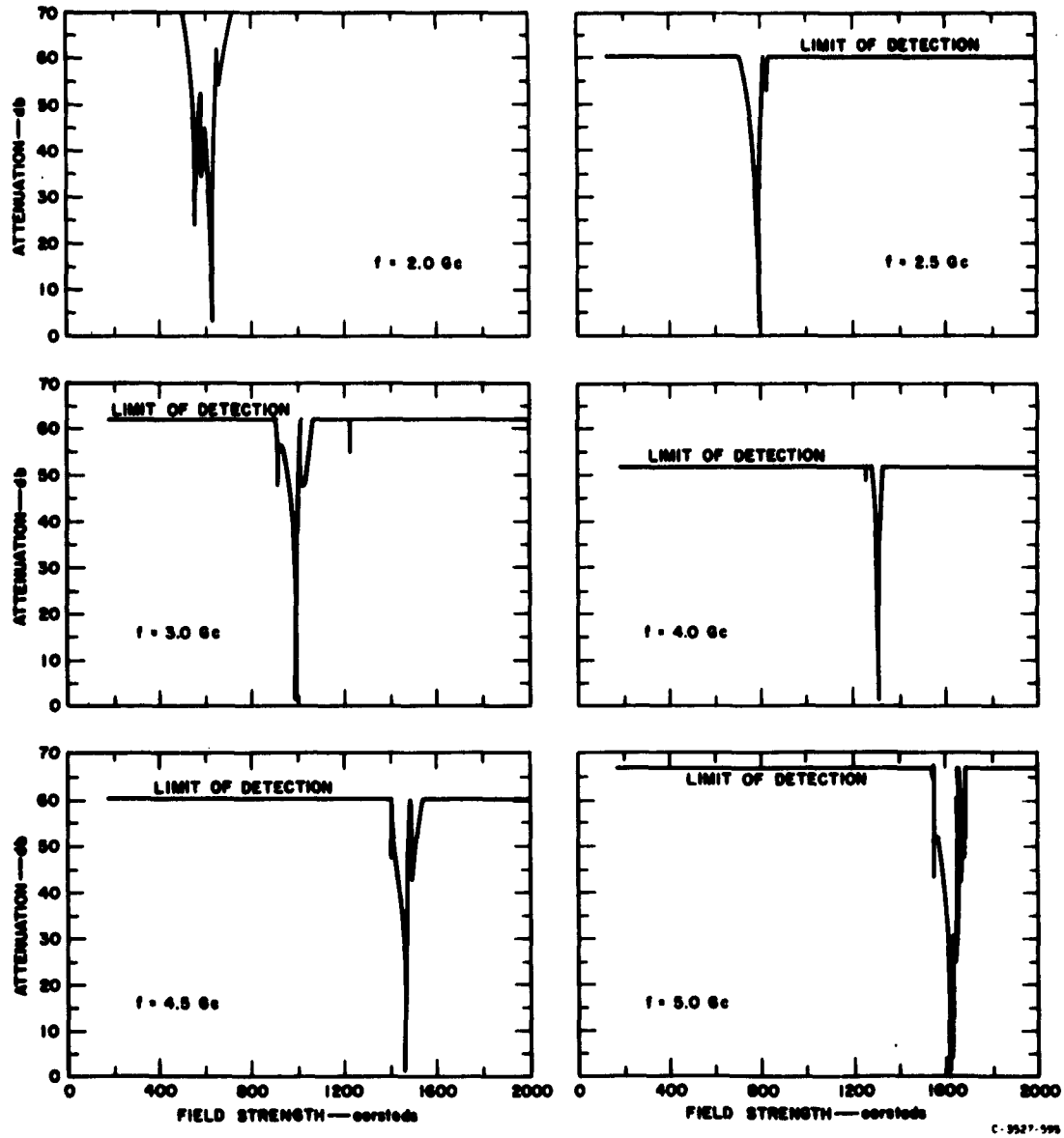

FIG. III G-4 THE STOP-BAND ATTENUATION CHARACTERISTICS vs. BIASING H-FIELD FOR THE FILTER IN FIG. III G-2

made with a swept magnetic field, measurements were made at various frequencies using fixed fields in order to accurately determine the frequency bandwidths at various tuning points and the mid-pass-band attenuation. These data are shown in Table III G-1. The responses shown in Fig. III G-4 were measured as the field was varied manually. No attempt was made to measure the exact shape of the various peaks of the main and spurious responses; the purpose of these plots was to show their position and intensity. In order to expedite the measurements in Fig. III G-4 the dc magnetic field was measured with a rotating coil gaussmeter (which has an absolute accuracy of only a few percent).

Table III G-1

CHARACTERISTICS OF THREE-RESONATOR FILTER

f_c (Gc)	$(L_A)_{min}$ (db)	$\Delta f^*_{3\ db}$ (Mc)	$\Delta f_{30\ db}$ (Mc)	VSWR	THEOR. $(L_A)_{min}$ (db)	H_0 (oersteds)
2.0	3.5	32.9*	91.4	2.50	--	610
2.5	1.7	34.2	90.1	--	--	867.1
3.0	1.7	33.6	90.6	1.23	1.57	990
4.0	1.4	30.9	87.2	1.10	1.7	1310
4.5	1.6	24.0	89.1	--	--	1586.8
7.0	1.6	29.6	--	--	--	--

* The bandwidths given are measured to the 3-db or 30-db point below $(L_A)_{min}$.

Perhaps the most important conclusion that was reached as a result of this study of a filter containing three resonators is that synchronous tuning can be maintained over a wide tuning range. This was accomplished by making the boundary conditions as similar as possible for the three resonators and then tuning out the remaining differences in resonant frequency by orienting the crystal axes with respect to the dc magnetic field. The band-center response curves indicate that the resonators "tracked" quite well all the way up to at least 7.0 Gc. It seems remarkable that this degree of synchronism was maintained over such a large tuning range when we observe that the electrical environment of the input and output resonators actually differs substantially from that of the center resonator. It can be inferred from these experimental results that it is probably possible to maintain synchronous tuning over a wide tuning range with an arbitrary number of resonators.

The factors which apparently limit the tuning range of this particular side-wall-coupled filter to frequencies under around 4.5 Gc are the spurious responses. These spurious responses in the f = 5.0 Gc attenuation characteristic can be seen in Fig. III G-4(f) and are undoubtedly due to higher-order magnetostatic modes. If these subsidiary peaks were due to detuning of the three resonators the attenuation at the band center would increase considerably; actually it remains quite low.

The spurious responses are most intense when they are close to the main resonance and are usually quite weak farther away from the band center. The reason for this is that the individual magnetostatic modes are coupled together weakly, due to propagation effects and the effects of the conducting boundaries of the filter, which cause the RF fields around the resonator to be non-uniform. Strong interaction occurs only when the resonant frequencies of the two modes are separated by a frequency difference which is very small compared with the average of the two resonant frequencies. An examination of the magnetostatic mode chart for a ferrimagnetic sphere[28] shows that many magnetostatic modes occur very close to the main (*i.e.*, uniform precession) resonance in the 4.5- to 5.5-Gc range. The mode chart[28] shows that they cross the uniform precession resonance moving from the low-frequency side to the high-frequency side of the uniform precession resonance as the uniform precession resonance frequency is increased by increasing the dc magnetic field. The degree of interaction between two modes is a function of the strength of the coupling between the modes and the Q's of the modes as well as the frequency separation between the modes. The degree of coupling thus depends on the degree to which the RF fields are distorted due to the conducting boundaries. Fletcher[31] has shown that the coupling between the modes which is due to propagation effects is proportional to $(kR_a)^2$ where k is the free space propagation constant, $2\pi/\lambda_0$, and R_a is the radius of the resonator. It is obvious from this fact, that it is desirable to keep the size of the resonator as small as possible both in order to minimize intermode coupling due to boundary effects and due to propagation effects.

Figures III G-4(a) to (f) indicate that this filter has an extremely high rejection at frequencies far removed from band center. At all center frequencies, the off-channel rejection was beyond the maximum value that could be measured with the available experimental setup. The lowest of

these values was 52 db at 4.0 Gc. At all other frequencies the off-channel was at least 60 db. Since the off-channel rejection is likely to be fairly insensitive to frequency, it is quite likely that the off-channel rejection is actually >60 db at all frequencies.

Table III G-1 shows the measured attenuation at band center and the VSWR at band center. The VSWR was low except at f_c = 2.0 Gc where, it is suspected, the resonators are undercoupled and are also slightly detuned. The measured dissipation loss values for this filter are also shown in Table III G-1. Alongside the measured values are those values of attenuation calculated from the response parameters [*i.e.*, bandwidth, degree of overcoupling, using Eq. (III B-4)] which would result if all three resonators had the same Q_u as was obtained with the two-resonator filter (see Fig. III C-2). The good agreement between these measured attenuation values and the values calculated from the two-resonator filter Q_u's shows that the filter is performing as might reasonably be expected. In fact the attenuation performance is somewhat better than might be expected when the slightly wider linewidth* of the center resonator (ΔH = 0.60 oer. at f = 4.4 Gc) is taken into consideration. Evidently the Q_u of the center resonator is not degraded by the center section conducting boundaries to the same degree as the input and output resonators are degraded by the strip-transmission line conducting boundaries.

The 30-db bandwidth of the filter stays quite constant over the tuning range, a fortuitous result for many applications. The ratio of the 30-db bandwidth to the 3-db bandwidth runs around 2.8 for the three-resonator filter design as compared to around 5 for the two-resonator filter design. Although the cutoff rate was considerably sharper for the three-resonator design, the performance of the three-resonator filter was probably not optimum in this respect because of a small amount of mistuning and because no effort was made to optimize the shape of the pass-band response for optimum rate of cutoff. Filters designed to correspond to equal-element prototypes[5] would probably be desirable for most tunable filter applications. Such filters would result in minimum midband dissipation loss for a given specified 30-db (or other specified level) stop-band width. In the case of the two- and three-resonator

* Measured in G-band full-height rectangular waveguide.

filters discussed herein, the three-resonator design has a 30-db bandwidth, which is about 23 percent less than that for the two-resonator design, but the three-resonator design has somewhat larger midband attenuation. By further optimization of the design, to correspond to an equal-element prototype, it should be possible to reduce the midband loss somewhat.

REFERENCES

1. C. N. Patel, "Magnetically Tunable Nonreciprocal Band-Pass Filters Using Ferrimagnetic Resonators," *IRE Trans. on Microwave Theory and Techniques, PGMTT*-10, 3,(May 1962).

2. L. K. Anderson, "Ferrimagnetic Relaxation Measurements and Microwave Circuit Properties of Ferrite Ellipsoids," Technical Note, Contract AF 49(638)-415, M.L. 880, Microwave Laboratory, W. W. Hansen Laboratories of Physics, Stanford University, Stanford, California (February 1962).

3. S. B. Cohn *et al.*, "Research on Design Criteria for Microwave Filters," Final Report SRI Project 1331, Contract DA 36-039 SC-64625, Stanford Research Institute, Menlo Park, California (June 1957).

4. G. L. Matthaei *et al.*, "Design Criteria for Microwave Filters and Coupling Structures," Chapter 13, Final Report, SRI Project 2326, Contract DA 36-039 SC-74862, Stanford Research Institute, Menlo Park, California (January 1961).

5. S. B. Cohn, "Dissipation Loss in Multiple-Coupled-Resonator Filters," *Proc. IRE* 47, pp. 1342-1348 (August 1959).

6. P. S. Carter, Jr., "Magnetically Tunable Microwave Filters Using Single-Crystal Yttrium-Iron-Garnet Resonators," *Trans. IRE PGMTT*-9, pp. 252-260 (May 1961).

7. P. S. Carter, Jr., C. Flammer, "Unloaded Q of Single Crystal Yttrium Iron-Garnet Resonator as a Function of Frequency," *IRE Trans. PGMTT*-9, 5 (September 1960).

8. E. G. Spencer and R. C. LeGraw, "Line Width Narrowing in Gallium-Substituted Yttrium-Iron-Garnet," *Bull. Am. Phys. Soc.*, Ser. 2, Vol. 5, Part 1, p. 58 (January 27, 1960).

9. J. W. Nielsen, D. A. Lepore, J. Zneimer, and G. B. Townsend, "Effect of Mechanical, Thermal, and Chemical Treatment of the Ferrimagnetic Resonance Linewidth on Lithium Ferrite Crystals," *Jour. Appl. Phys.*, 33S, *3* (March 1962).

10. C. P. Buffler, "Resonance Properties of Single-Crystal Hexagonal Ferrites," *Jour. Appl. Phys.* 33, *3* (March 1962).

11. S. Dixon, "High-Power Characteristics of Single-Crystal Ferrites with Planar Anisotropy," *Jour. Appl. Phys.*, 33S, *3* (March 1962).

12. Arthur Tauber, R. O. Savage, R. J. Gambino, and C. G. Whinfrey, "Growth of Single-Crystal Hexagonal Ferrites Containing Zn, *Jour. Appl. Phys.* 33S, *3* (March 1962).

13. P. J. B. Clarricoats, *Microwave Ferrites*, Chapter 2, pp 17-18, (John Wiley and Sons, Inc., New York, New York).

14. G. L. Matthaei, *et al.*, *op. cit.*, pp. 490-491.

15. W. A. Yager, J. K. Galt, F. R. Merritt, and E. A. Wood, "Ferromagnetic Resonance in Nickel Ferrite," *Phys. Rev.* 80, 4 (15 November 1950).

16. C. Kittel, "On The Theory of Ferromagnetic Resonance Absorption," *Phys. Rev.* 73, pp. 155-161 (1948).

17. J. O. Artman, "Microwave Resonance Relations in Anisotropic Single Crystals Ferrites," *Proc. IRE* 44, *10* (October 1956).

18. G. L. Matthaei, Leo Young, P. S. Carter, Jr., "Microwave Filters and Coupling Structures," Report No. 5, SRI Project 3527, Contract DA 36-039 SC-87398, Stanford Research Institute, Menlo Park, California (May 1962).

19. "Reference Data for Radio Engineers," 4th. ed., pp. 190-198 (International Telephone and Telegraph Corp., 1959).

20. P. H. Vartanian, W. P. Ayres, and A. L. Helgeason, "Propagation in Dielectric Slab-Loaded Rectangular Waveguide," *IRE Trans. PGMTT*-6, 2 (April 1958).

21. "Frequency-Selective Limiters Reduce Interference and Jamming," *Microwaves*, pp. 26-27 (September 1962).

22. R. W. DeGrasse, "Low-Loss Gyromagnetic Coupling Through Single Crystal Garnets," *Jour. Appl. Phys.*, Supplement to Vol. 30, No. 4 (April 1959).

23. R. Blow, "YIG Microwave Electronically Tunable Preselectors," *Microwave Journal* (May 1962).

24. P. S. Carter, Jr., *et al.*, "Microwave Filters and Coupling Structures," Third Quarterly Progress Report, Contract DA 36-039 SC-87398, SRI Project 3527, Stanford Research Institute, Menlo Park, California (October 1961).

25. W. J. Getsinger and G. L. Matthaei, "Microwave Filters and Coupling Structures," Second Quarterly Report, SRI Project 3527 Contract DA-36-039 SC-87398, Stanford Research Institute, Menlo Park, California (July 1961).

26. P. S. Carter, Jr., *et al.*, *op. cit.*, Table II-3.

27. I. H. Solt, Jr., and P. C. Fletcher, "Magnetic Anisotropy from the Magnetostatic Modes," *Jour. Appl. Phys.* 31S, 5 (May 1960).

28. P. C. Fletcher and R. O. Bell, "Ferrimagnetic Resonance Modes in Spheres," *Jour. Appl. Phys.* 30; 5 (May 1959).

29. J. W. Duncan, V. P. Minerva, "100:1 Bandwidth Balun Transformer," *Proc IRE* 48, 2 pp. 156-164 (February 1960).

30. E. M. T. Jones and J. T. Bolljahn, "Coupled-Strip-Transmission-Line Filters and Direction Couplers," *IRE Trans. PGMTT*-4, 2 (April 1956).

31. P. C. Fletcher and I. H. Solt, Jr., "Coupling of the Magnetostatic Modes," *Jour. Appl. Phys*, 30S, 4 (April 1959).

IV CONCLUSIONS

A. BAND-STOP FILTERS

The exact method for the design of band-stop filters discussed in Sec. II was demonstrated to be straightforward and potentially of great practical value. Even in the narrow-stop-band case, where an approximation was introduced by way of using reactively coupled stubs, very good accuracy in the stop-band width and the size of pass-band Tchebyscheff ripples was obtained. The straightforward design equations that were presented should make it possible for these design methods to be very widely used, since the design procedure is simple and requires little special knowledge.

B. MAGNETICALLY TUNABLE FILTERS WITH FERRIMAGNETIC RESONATORS

Reasonably good agreement has been obtained between the experimental data and the various design charts that were presented. Although the design procedures that were outlined involve a certain amount of cut and try in determining the sizes of coupling slots between spheres, experimental procedures appear to be unavoidable since the boundary value problem involved is very complex. The experimental procedures outlined provide a very practical approach to determining coupling iris size. However, the theoretical curves for finding the proper size of sphere to use in order to obtain a given external Q were found to be of considerable help in designing the input and output strip lines or waveguides.

The results in Sec. III show that magnetically tunable filters with almost any number of resonators should be possible. The tuning techniques described were shown to be practical, and the experimental results verify that the filter will stay in tune as the magnetic field is varied across a wide range.

ACKNOWLEDGMENTS

Mr. R. B. Larrick made the laboratory tests on the wide-band band-stop filter.

Mr. York Sato made the laboratory tests on the magnetically tunable filters, and contributed many ideas for the practical construction and testing of these filters.

PROGRAM FOR THE NEXT INTERVAL

It is anticipated that the work for the next interval will include:

(1) Further work on filters with magnetically tunable garnet resonators

(2) Further work on electronically tunable up-converters

(3) Further work on band-stop filters

(4) Further work on comb-line filters and loaded interdigital filters

(5) Further work on multiplexers

(6) Further work on the microwave filter book.

IDENTIFICATION OF KEY TECHNICAL PERSONNEL

	HOURS CHARGED TO PROJECT DURING QUARTER
DR. P. S. CARTER, JR. *Senior Research Engineer*	195
DR. E. G. CRISTAL *Research Engineer*	182
MR. W. J. GETSINGER *Senior Research Engineer*	8
DR. G. L. MATTHAEI *Manager, Electromagnetic Techniques Laboratory* *(Project Leader)*	241
MR. L. A. ROBINSON *Senior Research Engineer*	112.5
MR. B. M. SCHIFFMAN *Senior Research Engineer*	254
DR. LEO YOUNG *Senior Research Engineer*	180

On a sub-contract with TRG-West, Dr. E. M. T. Jones spent 96 hours during the quarter on the microwave filter book being prepared under this contract. Dr. Jones is writing certain portions of the book the research for which he worked on while employed at SRI. In addition, Stanford Research Institute and the authors have contributed additional work time toward the microwave filter book being written on this project.

DISTRIBUTION LIST

ORGANIZATION	NO. OF COPIES
Technical Library OASD (R and E) Room 3E1065, The Pentagon Washington 25, D. C.	1
Commanding Officer U.S. Army Signal Research and Development Agency Fort Monmouth, New Jersey Attn: SIGRA/SL-ADT	1
Commanding Officer U. S. Army Signal Research and Development Agency Fort Monmouth, New Jersey Attn: SIGRA/SL-ADJ (MP&R Unit No. 1, ECR Dept.)	1
Commanding Officer U. S. Army Signal Research and Development Agency Fort Monmouth, New Jersey Attn: SIGRA/SL-TN (FOR RETRANSMITTAL TO ACCREDITED BRITISH AND CANADIAN GOVERNMENT REPRESENTATIVES)	3
Commanding Officer U. S. Army Signal Research and Development Agency Fort Monmouth, New Jersey Attn: SIGRA/SL-LNF	3
Commanding Officer U. S. Army Signal Equipment Support Agency Fort Monmouth, New Jersey Attn: SIGMS/ADJ	1
Director U. S. Naval Research Laboratory Washington 25, D. C. Attn: Code 2027	1
Commanding Officer U.S. Army Signal Research and Development Agency Fort Monmouth, New Jersey Attn: SIGRA/SL	1
Commanding Officer and Director U. S. Navy Electronics Laboratory San Diego 52, California	1
U. S. Army Signal Liaison Office Aeronautical Systems Command Attn: ASDL-9 Wright-Patterson Air Force Base, Ohio	2
Commander Air Force Command and Control Development Division Air Research and Development Command U.S. Air Force Laurence G. Hanscom Field Bedford, Massachusetts Attn: CROTLR-2	1
Commander Rome Air Development Center Air Research and Development Command Griffiss Air Force Base, Rome, New York Attn: RCSSID	1
Commander Armed Services Technical Information Agency Arlington Hall Station Arlington 12, Virginia	10
Advisory Group on Electronic Parts Moore School Building 200 South 33rd Street Philadelphia 4, Pennsylvania	4
Commanding General Army Ordnance Missile Command Signal Office Redstone Arsenal, Alabama	1
Chief Bureau of Ships Department of the Navy Washington 25, D. C. Attn: 691B2C	1
Commander New York Naval Shipyard Materials Laboratory Brooklyn, New York Attn: CODE 910-d	1
Commanding Officer Diamond Ordnance Fuse Laboratories Washington 23, D. C. Attn: Technical Reference Section ORDTL-06.33	1
Commanding Officer Engineering Research and Development Laboratories Fort Belvoir, Virginia Attn: Technical Documents Center	1

DISTRIBUTION LIST

ORGANIZATION	NO. OF COPIES
Chief U. S. Army Security Agency Arlington Hall Station Arlington 12, Virginia	2
Deputy President U. S. Army Security Agency Board Arlington Hall Station Arlington 12, Virginia	1
MELABS Library Stanford Industrial Park 3300 Hillview Avenue Palo Alto, California	1
Airborne Instruments Laboratory Deer Park, Long Island, New York Attn: Mr. R. Sleven	1
Commanding Officer U. S. Army Signal Research Unit Mountain View, California Attn: SIGRU-3	1
Stanford Electronics Laboratory Stanford University Stanford, California Attn: Applied Electronics Laboratory	1
Convair Pomona, California	1
Commander Rome Air Development Center Griffiss Air Force Base Rome, New York Attn: RCLTM-2, Mr. Patsy A. Romanelli	1
Commanding Officer U. S. Army Signal Research and Development Agency Fort Monmouth, New Jersey Attn: SIGRA/SL-PRM (Mr. Reingold)	1
Rantec Corporation Calabasas, California Attn: S. B. Cohn Technical Director	1
U. S. Naval Ordnance Test Station China Lake, California Attn: Mr. Robert Corsine Code 4021	1
Technical Library General Electric Microwave Laboratory 601 California Avenue Palo Alto, California	1
Dr. K. L. Kotzebue Watkins-Johnson Company 3333 Hillview Avenue Stanford Industrial Park Palo Alto, California	1
Commanding Officer U. S. Army Signal Research and Development Agency Fort Monmouth, New Jersey Attn: SIGRA/SL-PEE (Mr. Wm. Dittilo)	22
Commanding Officer U. S. Army Signal Equipment Support Agency Fort Monmouth, New Jersey Attn: SIGMS/SDM	1
Polytechnic Institute of Brooklyn Route 110 Farmingdale, Long Island, New York Attn: Dr. Grieemaman	1

AD
STANFORD RESEARCH INSTITUTE, Menlo Park, California

MICROWAVE FILTERS AND COUPLING STRUCTURES, by B. M. Schiffman, P. S. Carter, Jr., G. L. Matthaei. Report 7, Seventh Quarterly Progress Report, 1 July to 30 September 1962, 77 pages, 39 Figs., 7 Tables, 43 Refs.

Contract DA 36-039 SC 87398, File No. 40553-PM-61-93-93, DA Project 3A99-15-002-02-06, SCL 2101N (14 July 1961)

An exact method is presented for the design of band-stop filters consisting of stubs and quarter-wavelength connecting lines. A low-pass prototype circuit is chosen, and the derived transmission-line band-stop filter has a response that is an exact mapping of the prototype response. The stop-band can have any width, but if it is very narrow, the stub impedances become unreasonable. It is then desirable to replace the stubs by capacitively or inductively coupled resonators of reasonable impedance, which introduces an approximation but gives good results. The design of filters with 3/4 spacings between resonators

UNCLASSIFIED

1. Microwave structures
2. Contract DA 36-039 SC 87398
3. Band-stop filters
4. Tunable filters

UNITERMS

electronic

microwave

tunable

circuit design

filter

ferrimagnetic

resonator

AD
STANFORD RESEARCH INSTITUTE, Menlo Park, California

MICROWAVE FILTERS AND COUPLING STRUCTURES, by B. M. Schiffman, P. S. Carter, Jr., G. L. Matthaei. Report 7, Seventh Quarterly Progress Report, 1 July to 30 September 1962, 77 pages, 39 Figs., 7 Tables, 43 Refs.

Contract DA 36-039 SC 87398, File No. 40553-PM-61-93-93, DA Project 3A99-15-002-02-06, SCL-2101N (14 July 1961)

An exact method is presented for the design of band-stop filters consisting of stubs and quarter-wavelength connecting lines. A low-pass prototype circuit is chosen, and the derived transmission-line band-stop filter has a response that is an exact mapping of the prototype response. The stop-band can have any width, but if it is very narrow, the stub impedances become unreasonable. It is then desirable to replace the stubs by capacitively or inductively coupled resonators of reasonable impedance, which introduces an approximation but gives good results. The design of filters with 3/4 spacings between resonators

UNCLASSIFIED

1. Microwave structures
2. Contract DA 36-039 SC 87398
3. Band-stop filters
4. Tunable filters

UNITERMS

electronic

microwave

tunable

circuit design

filter

ferrimagnetic

resonator

AD
STANFORD RESEARCH INSTITUTE, Menlo Park, California

MICROWAVE FILTERS AND COUPLING STRUCTURES, by B. M. Schiffman, P. S. Carter, Jr., G. L. Matthaei. Report 7, Seventh Quarterly Progress Report 1 July to 30 September 1962, 77 pages, 39 Figs., 7 Tables, 43 Refs.

Contract DA 36-039 SC 87398, File No. 40553-PM-61-93-93, DA Project 3A99-15-002-02-06, SCL-2101N (14 July 1961)

An exact method is presented for the design of band-stop filters consisting of stubs and quarter-wavelength connecting lines. A low-pass prototype circuit is chosen, and the derived transmission-line band-stop filter has a response that is an exact mapping of the prototype response. The stop-band can have any width, but if it is very narrow, the stub impedances become unreasonable. It is then desirable to replace the stubs by capacitively or inductively coupled resonators of reasonable impedance, which introduces an approximation but gives good results. The design of filters with 3/4 spacings between resonators

UNCLASSIFIED

1. Microwave structures
2. Contract DA 36-039 SC 87398
3. Band-stop filters
4. Tunable filters

UNITERMS

electronic

microwave

tunable

circuit design

filter

ferrimagnetic

resonator

AD
STANFORD RESEARCH INSTITUTE, Menlo Park, California

MICROWAVE FILTERS AND COUPLING STRUCTURES, by B. M. Schiffman, P. S. Carter, Jr., G. L. Matthaei. Report 7, Seventh Quarterly Progress Report 1 July to 30 September 1962, 77 pages, 39 Figs., 7 Tables, 43 Refs.

Contract DA 36-039 SC 87398, File No. 40553-PM-61-93-93, DA Project 3A99-15-002-02-06, SCL-2101N (14 July 1961)

An exact method is presented for the design of band-stop filters consisting of stubs and quarter-wavelength connecting lines. A low-pass prototype circuit is chosen, and the derived transmission-line band-stop filter has a response that is an exact mapping of the prototype response. The stop-band can have any width, but if it is very narrow, the stub impedances become unreasonable. It is then desirable to replace the stubs by capacitively or inductively coupled resonators of reasonable impedance, which introduces an approximation but gives good results. The design of filters with 3/4 spacings between resonators

UNCLASSIFIED

1. Microwave structures
2. Contract DA 36-039 SC 87398
3. Band-stop filters
4. Tunable filters

UNITERMS

electronic

microwave

tunable

circuit design

filter

ferrimagnetic

resonator

is also discussed; it is of interest for the design of waveguide band-stop filters where it is desired to avoid interaction between fringing fields at the coupling irises. The procedure used in establishing parameters and dimensions of magnetically tunable filters is reviewed, with charts and graphs that enable a designer to find the dimensions of the circuit elements, including ferrimagnetic resonators, to give a specified band-pass frequency response. Promising circuit structures are presented, and two design examples are given. Performances of two side-wall-coupled strip-line filters, one with two resonators and the other with three, are given.	UNCLASSIFIED	is also discussed; it is of interest for the design of waveguide band-stop filters where it is desired to avoid interaction between fringing fields at the coupling irises. The procedure used in establishing parameters and dimensions of magnetically tunable filters is reviewed, with charts and graphs that enable a designer to find the dimensions of the circuit elements, including ferrimagnetic resonators, to give a specified band-pass frequency response. Promising circuit structures are presented, and two design examples are given. Performances of two side-wall-coupled strip-line filters, one with two resonators and the other with three, are given.	UNCLASSIFIED
is also discussed; it is of interest for the design of waveguide band-stop filters where it is desired to avoid interaction between fringing fields at the coupling irises. The procedure used in establishing parameters and dimensions of magnetically tunable filters is reviewed, with charts and graphs that enable a designer to find the dimensions of the circuit elements, including ferrimagnetic resonators, to give a specified band-pass frequency response. Promising circuit structures are presented, and two design examples are given. Performances of two side-wall-coupled strip-line filters, one with two resonators and the other with three, are given.	UNCLASSIFIED	is also discussed; it is of interest for the design of waveguide band-stop filters where it is desired to avoid interaction between fringing fields at the coupling irises. The procedure used in establishing parameters and dimensions of magnetically tunable filters is reviewed, with charts and graphs that enable a designer to find the dimensions of the circuit elements, including ferrimagnetic resonators, to give a specified band-pass frequency response. Promising circuit structures are presented, and two design examples are given. Performances of two side-wall-coupled strip-line filters, one with two resonators and the other with three, are given.	UNCLASSIFIED

AD
STANFORD RESEARCH INSTITUTE, Menlo Park, California

MICROWAVE FILTERS AND COUPLING STRUCTURES, by B. M. Schiffman, P. S. Carter, Jr., G. L. Matthaei. Report 7, Seventh Quarterly Progress Report, 1 July to 30 September 1962, 77 pages, 39 Figs., 7 Tables, 43 Refs.

Contract DA 36-039 SC 87398, File No. 40553-PM-61-93-93, DA Project 3A99-15-002-02-06, SCL 2101N (14 July 1961)

An exact method is presented for the design of band-stop filters consisting of stubs and quarter-wavelength connecting lines. A low-pass prototype circuit is chosen, and the derived transmission-line band-stop filter has a response that is an exact mapping of the prototype response. The stop-band can have any width, but if it is very narrow, the stub impedances become unreasonable. It is then desirable to replace the stubs by capacitively or inductively coupled resonators of reasonable impedance, which introduces an approximation but gives good results. The design of filters with 3/8 spacings between resonators

UNCLASSIFIED

1. Microwave structures
2. Contract DA 36-039 SC 87398
3. Band-stop filters
4. Tunable filters

UNITERMS

electronic

microwave

tunable

circuit design

filter

ferrimagnetic

resonator

AD
STANFORD RESEARCH INSTITUTE, Menlo Park, California

MICROWAVE FILTERS AND COUPLING STRUCTURES, by B. M. Schiffman, P. S. Carter, Jr., G. L. Matthaei. Report 7, Seventh Quarterly Progress Report, 1 July to 30 September 1962, 77 pages, 39 Figs., 7 Tables, 43 Refs.

Contract DA 36-039 SC 87398, File No. 40553-PM-61-93-93, DA Project 3A99-15-002-02-06, SCL-2101N (14 July 1961)

An exact method is presented for the design of band-stop filters consisting of stubs and quarter-wavelength connecting lines. A low-pass prototype circuit is chosen, and the derived transmission-line band-stop filter has a response that is an exact mapping of the prototype response. The stop-band can have any width, but if it is very narrow, the stub impedances become unreasonable. It is then desirable to replace the stubs by capacitively or inductively coupled resonators of reasonable impedance, which introduces an approximation but gives good results. The design of filters with 3/8 spacings between resonators

UNCLASSIFIED

1. Microwave structures
2. Contract DA 36-039 SC 87398
3. Band-stop filters
4. Tunable filters

UNITERMS

electronic

microwave

tunable

circuit design

filter

ferrimagnetic

resonator

AD
STANFORD RESEARCH INSTITUTE, Menlo Park, California

MICROWAVE FILTERS AND COUPLING STRUCTURES, by B. M. Schiffman, P. S. Carter, Jr., G. L. Matthaei. Report 7, Seventh Quarterly Progress Report 1 July to 30 September 1962, 77 pages, 39 Figs., 7 Tables, 43 Refs.

Contract DA 36-039 SC 87398, File No. 40553-PM-61-93-93, DA Project 3A99-15-002-02-06, SCL-2101N (14 July 1961)

An exact method is presented for the design of band-stop filters consisting of stubs and quarter-wavelength connecting lines. A low-pass prototype circuit is chosen, and the derived transmission-line band-stop filter has a response that is an exact mapping of the prototype response. The stop-band can have any width, but if it is very narrow, the stub impedances become unreasonable. It is then desirable to replace the stubs by capacitively or inductively coupled resonators of reasonable impedance, which introduces an approximation but gives good results. The design of filters with 3/8 spacings between resonators

UNCLASSIFIED

1. Microwave structures
2. Contract DA 36-039 SC 87398
3. Band-stop filters
4. Tunable filters

UNITERMS

electronic

microwave

tunable

circuit design

filter

ferrimagnetic

resonator

AD
STANFORD RESEARCH INSTITUTE, Menlo Park, California

MICROWAVE FILTERS AND COUPLING STRUCTURES, by B. M. Schiffman, P. S. Carter, Jr., G. L. Matthaei. Report 7, Seventh Quarterly Progress Report, 1 July to 30 September 1962, 77 pages, 39 Figs., 7 Tables, 43 Refs.

Contract DA 36-039 SC 87398, File No. 40553-PM-61-93-93, DA Project 3A99-15-002-02-06, SCL-2101N (14 July 1961)

An exact method is presented for the design of band-stop filters consisting of stubs and quarter-wavelength connecting lines. A low-pass prototype circuit is chosen, and the derived transmission-line band-stop filter has a response that is an exact mapping of the prototype response. The stop-band can have any width, but if it is very narrow, the stub impedances become unreasonable. It is then desirable to replace the stubs by capacitively or inductively coupled resonators of reasonable impedance, which introduces an approximation but gives good results. The design of filters with 3/8 spacings between resonators

UNCLASSIFIED

1. Microwave structures
2. Contract DA 36-039 SC 87398
3. Band-stop filters
4. Tunable filters

UNITERMS

electronic

microwave

tunable

circuit design

filter

ferrimagnetic

resonator

is also discussed; it is of interest for the design of waveguide band-stop filters where it is desired to avoid interaction between fringing fields at the coupling irises. The procedure used in establishing parameters and dimensions of magnetically tunable filters is reviewed, with charts and graphs that enable a designer to find the dimensions of the circuit elements, including ferrimagnetic resonators, to give a specified band-pass frequency response. Promising circuit structures are presented, and two design examples are given. Performances of two side-wall-coupled strip-line filters, one with two resonators and the other with three, are given.	UNCLASSIFIED	is also discussed; it is of interest for the design of waveguide band-stop filters where it is desired to avoid interaction between fringing fields at the coupling irises. The procedure used in establishing parameters and dimensions of magnetically tunable filters is reviewed, with charts and graphs that enable a designer to find the dimensions of the circuit elements, including ferrimagnetic resonators, to give a specified band-pass frequency response. Promising circuit structures are presented, and two design examples are given. Performances of two side-wall-coupled strip-line filters, one with two resonators and the other with three, are given.	UNCLASSIFIED
is also discussed; it is of interest for the design of waveguide band-stop filters where it is desired to avoid interaction between fringing fields at the coupling irises. The procedure used in establishing parameters and dimensions of magnetically tunable filters is reviewed, with charts and graphs that enable a designer to find the dimensions of the circuit elements, including ferrimagnetic resonators, to give a specified band-pass frequency response. Promising circuit structures are presented, and two design examples are given. Performances of two side-wall-coupled strip-line filters, one with two resonators and the other with three, are given.	UNCLASSIFIED	is also discussed; it is of interest for the design of waveguide band-stop filters where it is desired to avoid interaction between fringing fields at the coupling irises. The procedure used in establishing parameters and dimensions of magnetically tunable filters is reviewed, with charts and graphs that enable a designer to find the dimensions of the circuit elements, including ferrimagnetic resonators, to give a specified band-pass frequency response. Promising circuit structures are presented, and two design examples are given. Performances of two side-wall-coupled strip-line filters, one with two resonators and the other with three, are given.	UNCLASSIFIED

STANFORD RESEARCH INSTITUTE

MENLO PARK
CALIFORNIA

Regional Offices and Laboratories

Southern California Laboratories
820 Mission Street
South Pasadena, California

Washington Office
808 17th Street, N.W.
Washington 5, D.C.

New York Office
270 Park Avenue, Room 1770
New York 17, New York

Detroit Office
The Stevens Building
1025 East Maple Road
Birmingham, Michigan

European Office
Pelikanstrasse 37
Zurich 1, Switzerland

Japan Office
911 Iino Building
22, 2-chome, Uchisaiwai-cho, Chiyoda-ku
Tokyo, Japan

Representatives

Honolulu, Hawaii
Finance Factors Building
195 South King Street
Honolulu, Hawaii

London, England
19 Upper Brook Street
London, W. 1, England

Milan, Italy
Via Macedonio Melloni 40
Milano, Italy

London, Ontario, Canada
P.O. Box 762
London, Ontario, Canada